REMOVAL OF As(V) CONTAMINATED WATER BY A COMBINATION OF

ZERO-VALENT IRON COATED SAND AND IRON OXIDE-COATED SAND

USED IN PERMEABLE REACTIVE BARRIER

Miss Chonnikarn Amasvata

A Thesis Submitted in Partial Fulfillment of the Requirements

for the Degree of Master of Science Program in Environmental Management

(Interdisciplinary Program)

Graduate School

Chulalongkorn University

Academic Year 2014

การกำจัดสารอาร์เซเนตในน้ำปนเปื้อนโดยใช้
Zero-valent iron coated sand ร่วมกับ iron oxide-coated sand
ในผนังพรุนที่ทำปฏิกิริยากับมลสาร

นางสาวชนนิกานต์ อมัตวะตะ

Thesis Title	REMOVAL OF As(V) CONTAMINATED WATER BY A COMBINATION OF ZERO-VALENT IRON COATED SAND AND IRON OXIDE-COATED SAND USED IN PERMEABLE REACTIVE BARRIER
By	Miss Chonnikarn Amasvata
Field of Study	Environmental Management
Thesis Advisor	Assistant Professor Srilert Chotpantarat, Ph.D.

Accepted by the Graduate School, Chulalongkorn University in Partial Fulfillment of the Requirements for the Master's Degree

⋯⋯⋯⋯⋯⋯⋯⋯⋯⋯⋯⋯⋯⋯⋯⋯Dean of the Graduate School

(Associate Professor Sunait Chutintaranond, Ph.D.)

THESIS COMMITTEE

⋯⋯⋯⋯⋯⋯⋯⋯⋯⋯⋯⋯⋯⋯⋯Chairman

(Assistant Professor Chantra Tongcumpou, Ph.D.)

⋯⋯⋯⋯⋯⋯⋯⋯⋯⋯⋯⋯⋯⋯⋯Thesis Advisor

(Assistant Professor Srilert Chotpantarat, Ph.D.)

⋯⋯⋯⋯⋯⋯⋯⋯⋯⋯⋯⋯⋯⋯⋯Examiner

(Associate Professor Patiparn Punyapalakul, Ph.D.)

⋯⋯⋯⋯⋯⋯⋯⋯⋯⋯⋯⋯⋯⋯⋯Examiner

(Pichet Chaiwiwatworakul, Ph.D.)

⋯⋯⋯⋯⋯⋯⋯⋯⋯⋯⋯⋯⋯⋯⋯External Examiner

(Associate Professor Wasant Pongsapich, Ph.D.)

ชนนิกานต์ อมัตวะตะ : การกำจัดสารอาร์เซเนตในน้ำปนเปื้อนโดยใช้Zero-valent iron coated sand ร่วมกับ iron oxide-coated sand ในผนังพรุนที่ทำปฏิกิริยากับมลสาร (REMOVAL OF As(V) CONTAMINATED WATER BY A COMBINATION OF ZERO-VALENT IRON COATED SAND AND IRON OXIDE-COATED SAND USED IN PERMEABLE REACTIVE BARRIER) อ.ที่ปรึกษาวิทยานิพนธ์หลัก: ผศ.ดร. ศรีเลิศ โชติพันธ รัตน์, 86 หน้า.

งานวิจัยนี้ทำการศึกษาการกำจัดสารอาร์ซิเนตในน้ำใต้ดินโดยทำการทดลองแบบคอลัมน์ งานวิจัยได้ประยุกต์ใช้วัสดุดูดซับที่แตกต่างกัน 3 ชนิด โดยแบ่งการทดลองออกเป็น 6 คอลัมน์ ประกอบด้วย ทราย เหล็กออกไซด์เคลือบทราย และเหล็กประจุศูนย์เคลือบทราย (ZVICS) ผสมกับเหล็กออกไซด์เคลือบทราย (IOCS) ภายใต้สภาวะ pH ที่แตกต่างกัน (pH 4 และ 7) เพื่อเปรียบเทียบความสามารถในการดูดซับสารอาร์ซิเนตโดยตัวดูดซับที่แตกต่าง กันและที่ pH ที่แตกต่างกัน ผลการทดลองพบว่าความสามารถในการดูดซับสารอาร์ซิเนตผ่านคอลัมน์ที่ผสมระหว่าง เหล็กประจุศูนย์เคลือบทราย (ZVICS) ผสมกับเหล็กออกไซด์เคลือบทราย (IOCS) มีปริมาณมากกว่าเหล็กออกไซด์เคลือบทราย (IOCS) และทรายที่ pH 4 และ pH 7 ดังนี้ : 0.0328 mg As/g > 0.024 mg As/g > 0.014 mg As/g (ที่ pH 4),0.0135 mg As/g > 0.0115 mg As/g > 0.0064 mg As/g (ที่ pH 7) ตามลำดับ ผลการทดลองพบว่าความสามารถในการดูดซับสารอาร์ซิเนตมีค่าเพิ่มขึ้น เมื่อค่า pH ของสารละลายมีค่าน้อยลง นอกจากนี้ค่า pH_{zpc} ของทราย เหล็กออกไซด์เคลือบทราย และเหล็กศูนย์เคลือบทรายผสมกับเหล็กออกไซด์เคลือบทรายมีค่าเท่ากับ 5±0.03, 7±0.02 and 7.5±0.3 ตามลำดับ ประจุบนพื้นผิวของวัสดุดูดซับจะแสดงประจุบวกเมื่อสารละลายมีค่า pH น้อยกว่าค่า pH_{zpc} และจะแสดงประจุลบเมื่อสารละลายมีค่า pH มากกว่า pH_{zpc} ดังนั้นประจุบนพื้นที่ผิวของตัวดูดซับจึงมีผลกระทบต่อการดูดซับของสารอาร์ซิเนตบนพื้นที่ผิวตัวดูดซับ นอกจากนี้ผลของความสามารถในการดูดซับสารอาร์ซิเนตยังสามารถบอกได้ว่าการ เคลือบพื้นผิวทรายด้วยเหล็กออกไซด์และเหล็กศูนย์สามารถเพิ่มพื้นที่ผิวต่อ การดูดซับสารอาร์ซิเนตได้ ลักษณะพื้นที่ผิวของวัสดุดูดซับและปริมาณธาตุบนพื้นที่ผิววิเคราะห์ด้วย เครื่อง X-ray spectroscopy (SEM-DEX) Energy Dispersive X-Ray Spectrometer(EDX/EDS) พบสารอาร์ซิเนตเกาะอยู่บนตัวดูดซับทั้ง 3 ชนิด ผลจากการสกัดอาร์ซิเนตจากพื้นที่ผิวตัวดูดซับทั้ง 3 ชนิดพบว่า ปริมาณอาร์ซิเนตที่ดูดซับอยู่บนพื้นที่ผิว ที่ผสมระหว่าง เหล็กศูนย์เคลือบทรายและเหล็กออกไซด์เคลือบทราย มีปริมาณมากกว่าคอลัมน์เหล็กออกไซด์เคลือบทราย และคอลัมน์ทราย นอกจากนี้ยังพบว่ากระบวนการดูดซับสารอาร์ซิเนตบนผิวทรายสอดคล้องกับแบบจำลอง uniform (equilibrium) solute transport model ในทางกลับกันกระบวนการดูดซับสารอาร์ซิเนตบนผิวคอลัมน์ที่ผสมระหว่างเหล็ก ศูนย์เคลือบทรายและเหล็กออกไซด์เคลือบทราย และคอลัมน์เหล็กออกไซด์เคลือบทรายสอดคล้องกับแบบจำลอง chemical non-equilibrium two-site model (TSM).

สาขาวิชา การจัดการสิ่งแวดล้อม	ลายมือชื่อนิสิต	....
ปีการศึกษา 2557	ลายมือชื่อ อ.ที่ปรึกษาหลัก	....

5587678820 : MAJOR ENVIRONMENTAL MANAGEMENT

KEYWORDS: ARSENIC(V) REMOVAL / IRON OXIDE-COATED SAND / COLUMN EXPERIMENT / ZERO-VALENT IRON COATED SAND

CHONNIKARN AMASVATA: REMOVAL OF As(V) CONTAMINATED WATER BY A COMBINATION OF ZERO-VALENT IRON COATED SAND AND IRON OXIDE-COATED SAND USED IN PERMEABLE REACTIVE BARRIER. ADVISOR: ASST. PROF. SRILERT CHOTPANTARAT, Ph.D., 86 pp.

This research aims to evaluate the removal efficiency of As(V) contaminated in groundwater in different reactive materials under acidic and neutral conditions by using column experiments. Six columns were set up for As(V) removal efficiency with three different materials, used as the reactive barrier media packed in columns, under different pH (e.g., pH 4 and 7) conditions. The reactive materials consist of pure sand (control column), iron oxide coated sand (IOCS) and the combination of IOCS and zero-valent iron coated sand (ZVICS). According to column experiments, the descending orders of removal capacity (mg As/g) under pH 4 and 7 by combination of ZVICS and IOCS, IOCS and sand are: 0.0328 mg As/g > 0.024 mg As/g > 0.014 mg As/g as well as 0.0135 mg As/g > 0.0115 mg As/g > 0.0064 mg As/g, respectively. The results of column experiments showed that the removal of As(V) increase with decreasing pH. The pH_{zpc} of sand, IOCs and ZVICS-IOCS (i.e., 5±0.03, 7±0.02 and 7.5±0.3) affect to removal capacity of As(V) on different reactive materials. Moreover, that coating sand with iron oxide and zero-valent (ZVI) cause an increase of pore site, causing specific surface areas appear to be more available for the As(V) sorption. The SEM images and the corresponding EDX spectrum of acid-washed natural sand, IOCS and ZVICS with IOCS before and after finished As(V) transport through columns at pH 4 and pH 7 found As(V) adsorption onto all reactive material. The results of microwave digestion indicated that the As(V) retained on the mixing of ZVICS and IOCS more than IOCS and sand column. The mechanism of As(V) adsorption onto sand at pH 4 and pH 7 correspond to the uniform (equilibrium) solute transport model. On the contrary, IOCS and ZVICS-IOCS at pH 4 and pH 7 correspond to chemical non-equilibrium two-site model (TSM).

Field of Study: Environmental Management   Student's Signature ....

Academic Year: 2014   Advisor's Signature ....

ACKNOWLEDGEMENTS

CONTENTS

LIST OF TABLES

LIST OF FIGURES

จุฬาลงกรณ์มหาวิทยาลัย
CHULALONGKORN UNIVERSITY

CHAPTER 1

INTRODUCTION

1.1 Rational

Arsenic (As) can contaminate with the environment via natural processes (e.g. erosion and weathering processes of soil, minerals, and ores) and human activities (e.g. mining activities, combustion of fossil fuels, and use of pesticides and herbicides) (Nova scotia environment, 2008). Arsenic is mostly found in groundwater wells. Its occurrence in groundwater depends on types of rock and soil in the areas.

Regarding the increased concentrations of As in natural water, there are many areas in the world, including some areas in Thailand, where arsenic is found in higher concentrations than the World Health Organization (WHO) guideline of 10 µg/L (WHO, 1993). For example, (Choprapawon et al., 1999) studied the impact of As in Ronpibool District, Nakorn Sri Thammarat, the southern province of Thailand in the past ten years. The provincial administrative organization and the dweller of this district had recognized the harmful from As contamination in natural water sources in Ronpibool District for more than 10 years. This study aimed to control the chronic As poisoning which cause the illnesses to the resident in this district. Moreover, In the area surrounding gold mine at Wangsaphung District, Loei province, Northeast Thailand, in 2006, the villagers who live around this area complained about contamination of As in

the natural water source caused by mining activities. They found significant high level of As in soils, water and plants in neighborhood of the gold mine area that might cause an impact on their health in the future (Weerasiri et al., 2012). This has become an issue, because groundwater has been increasingly used for drinking water production in many countries.

The As contaminated in drinking water has caused seriously adverse effects, both in short and long terms to human's health and other living organisms. Short-term exposure (over days or weeks) in high levels of As in drinking water could result in nausea, diarrhea, and muscle pain. Furthermore, long-term exposure (over years or decades) in high level of As in drinking water could result in skin changes, damages to major body organs and some types of cancer (Nova scotia environment, 2008).

High concentration of As are found in groundwater in both oxidizing and reducing condition. The presence of As in oxidizing condition generally occurs in form of As(V) while in reducing condition mainly occurs in form of As(III). A few years ago, the problem of increasing As concentration in Thailand usually occur around mining area. Under the generally acid conditions around the mining area found high concentration of As combined with other elements is commonly found in lethal amount. The oxidation of asenopyrite (Fe_2SAS) leads to sulfuric acid and releases of As in unsaturated zone, which is source of Acid mine drainage (AMD). As in unsaturated zone mostly occur in form As(III). However, As(III) in groundwater can activated by mining activity cause O_2 exposed to unconfined shallow aquifer and As(III) can be

oxidizing to As(V). Thus, greater attention is must be focused on the process for removal of As(V) from groundwater.

This thesis focuses on threating As(V) that occurs in the unconfined shallow aquifer. Zero-valent iron (ZVI) has a good quality reactive material that mostly used as a permeable reactive barrier (PRB) for remediation of As contaminated in groundwater. In the recent year, the studied (Mak et al., 2011) found that ZVI has a high removal capacity for removal of As contaminated in water. However, these removal capacities might cause the formation of an iron oxyhydroxide corrosion product which may release As back into solution under prolonged anoxic condition (Han et al., 2011). Moreover, ZVI can be oxidized by water itself. If these reaction occur associated with the reduction of hydrogen and nitrate gas as a result in hydrongen and dinitrogen occur in the system (Henderson and Demond, 2011; Kamolpornwijit et al., 2003; Zhang and Gillham, 2005). As a result of the precipitation of solids and the formation of gases from oxidation and reduction of ZVI can drop the permeability of a permeable reactive barrier (PRB) and causing the hydraulic failure. Although, ZVI have disadvantage but it have an advantage when mixing it with iron oxide-coated sand (IOCS). (Mak et al., 2011) studied the removal of co-present Cr(VI) and As(V) by using a combination of zero-valent iron (Fe^0) and iron oxide-coated sand (IOCS). They found that the adsorption of As(V) was mainly absorbed onto IOCS and Fe^0 corrosion products while Cr(VI) was mainly absorbed onto Fe^0 and its corrosion products. Moreover, the studied found using the mixing of Fe^0 and IOCS as a reactive material for removal Cr(VI) and As(V) has

a high removal efficiencies and could be better use in permeable reactive barrier (PRBs) for removing Cr(VI) and As(V) from groundwater contaminant.

A few years ago, innovative technologies, such as coating of iron-oxide coat onto the surfaces of sand was interested because it's has a higher efficiencies for removal heave metals contaminated (i.e. Cr(VI), Pb(II), Cu(II), As(III)) have been used by many researchers (Dhagat et al., 2013; Eisazadeh et al., 2013; Gupta et al., 2005 Han et al., 2006). The study about using reactive material for removal heavy metals in the past focused on batch experiment more than on column experiment. Such batch experiment cannot deeply explain long term effect of As(V) removal onto reactive media (e.g. IOCS and/or ZVICS), which normally happens in column experiments. Moreover, there are a few studies about removal of As(V) by IOCS in combination with ZVICS by using column experiments. In order to get a better understanding on long-term sorption behavior of IOCS only and a combination of ZVICS and IOCS for As(V) removal under different pHs

Therefore, this study aims: (1) to evaluate the As(V) removal efficiency in contaminated water by combination of IOCS and ZVICS and (2) to describe the effect of pHs on As(V) removal in different reactive materials. The research applied three different reactive materials under different pHs (pH 4 and pH 7), containing in six columns. The reactive materials consist of pure sand (control column), IOCS, column and the combination of IOCS and ZVICS column in comparing arsenic (V) removal efficiency in column experiments.

1.2 Objectives

- To investigate the effect of pH (4 and 7) on As(V) removal in different reactive materials (Sand, IOCS and ZVICS in combination with IOCS)

- To evaluate the As(V) removal capacity by combination of ZVICS and IOCS compared with IOCS only in column and sand column

1.3 Hyprothesis

- Mixing of ZVICS and IOCS will increase As(V) removal capacity compared with those of IOCS or sand.

1.4 Scope of study

This thesis focuses on removal As(V) contaminated water. The research applied three different reactive materials under different pHs (pH 4 and pH 7), containing in six columns. The reactive materials consist of pure sand (control column), IOCS, column and the combination of IOCS and ZVICS column in comparing arsenic (V) removal efficiency in column experiments.

CHAPTER II

LITERATURE REVIEW AND THEORETICAL BACKGROUND

Groundwater is a source of drinking water that many countries in the world use for consumption because of groundwater has good quality and is cleaner than surface water. Anyway, groundwater occasionally contaminated with heavy metals such as Fe, As, Cd, Mn and other impurity. The existence of these contaminants in groundwater has adverse effects on human's health and other living. In many parts of the world found As contaminated in groundwater (Petrusevski et al, 2007). The only way to protect the toxicity of As contaminated in drinking water is to use arsenic-free water source or treat the arsenic from drinking water. The acceptable As concentration that prescribed by the World Health Organization (WHO) guideline is not higher than 10 µg/l (WHO, 2006). Moreover, in many parts of the world found the concentration of As was less, equal or higher than the WHO guideline. The As released to groundwater causing natural phenomena and anthropogenic activities. The natural phenomena such as volcanic emissions, weathering reactions, geochemical reactions and biological activities and also by anthropogenic activities, such as mining activities, use of arsenic pesticides and herbicides, combustion of fossil fuels, and adding crop desiccant (Mohan et al., 2007). If consumers know about how As released to groundwater, It will help us to avoid the As contaminated resources and will suggest appropriate treatments for the contaminated sources. There are many techniques for As removal

from drinking water such as enhanced coagulation, reverse osmosis, nano filtration, ion exchange, in-situ subsurface arsenic removal, adsorption by activated alumina, adsorption by iron-oxide coated sand, granular ferric hydroxide and other adsorbents (Petrusevski et al, 2008). The factor for choosing the best techniques for As removal depending on removal cost-effectiveness, efficiency of the technique, the appropriateness of technique for applying in contaminated area, and facility of the technique.

In recent years, use of IOCS and other materials for coated onto grains sand is very interesting. The adsorption efficiency of arsenic onto IOCs by using batch experiment shows the IOCS have high removal capacity of both As(III) and As(V) at lower pH condition and the studied found the As(V) adsorption increased with decreasing pH (Hsu et al., 2008).

Gupta et al. (2005) studied the removal of As(III) on IOCS compared with uncoated sand in batch and column studies, which carry out under a various range of pH, time, initial As(III) concentration and adsorbent dosage.

In batch experiment with the lower concentration of As(III) (100 µg/L) the removal efficiencies of As(III) was 99%. The results found that the removal efficiencies of As(III) decrease with increase initial As(III) concentrations. At the higher concentration of As(III) (800 µg/l) the maximum removal efficiencies of As(III) were about 75% and 6%, respectively for coated sand and uncoated sand. The reason that why the adsorption efficiency of As(III) decreased when increased initial As(III) concentrations

may be owing to As(III) adsorbed onto the adsorbent sites until the adsorption site become saturated. The Langmuir sorption isotherm was used for the estimated of maximum As(III) uptake (X_m) at different initial As(III) concentrations. The adsorption capacity (X_m) was decreased from 28.57 µg/g to 5.63 µg/g, respectively. The results show that the As(III) adsorption onto IOCS higher than that of the uncoated sand. Moreover, the study the effect of adsorbent dose on As(III) uptake shows that when increase the adsorbent dose from 5 g/L to 20 g/L adsorption efficiency of As(III) onto IOCS increases rapidly. At 20 g/L of adsorbent dose, The As(III) removal efficiencies decreased from 94% and 12.5%, respectively in the case of coated sand compared with uncoated sand. The results show that the As(III) adsorption onto IOCS increases with increase of the adsorbent dose because more adsorbent surface is available for the As(III) to be adsorbed.

Column experiment studied the effect of flow rate varied with time on the adsorption of As(III) onto IOCS and uncoated sand. In the case of coated sand (IOCS), when increasing the flow rate from 4 ml/min to 7 ml/min of 2 hours the adsorption of As(III) onto IOCS was decreased from 94% to 76% and increased to 92 with increasing contact time of 3 hours. Similarly, in the case of uncoated sand the results observed the maximum As(III) removal was 46% at the flow rate of 4 ml/min in 2 hours and decrease to 33% and 24% with increase flow rate to 7 ml/min and 10 ml/min, respectively. The results show that an increase in flow rate effect to decreasing the removal efficiency of As(III) in both case of coated sand and uncoated sand.

Vaishya and Gupta (2006) studies the As(V) removal by sulfate-modified IOCS (SMIOCS) in a fixed bed column. The results of the fixed bed study indicates that As(V) removal in fixed pH solution was 7.5, the size of sorbent was 498 µm and influent As concentrations was 1.0 mg/L. The results showed that the particle size of adsorbent effect to the As(V) adsorption onto adsorption site, the smaller particles have more adsorption site for adsorbed As(V) onto surface than larger particles. In the alkalinity and hardness condition the breakthrough time of the reactor was increase. In the contrary, in the acidic condition found the higher solid phase on the SMIOCS surface. Sodium hydroxide (NaOH) proves to be an efficient elutant for desorption of As(V) from SMIOCS in the column experiment.

Gebreyowhannes (2009) studied the effect of silica and pH on As(III) removal by IOCS in batch experiments. The results show at IOCS dosage of 0.2 g/L and 0.3 g/L with contact time 24 hours the As(V) removal efficiency was above 85% and increase to higher than 97% when increasing of IOCS dosage to 1.0 g/L, 1.5 g/L and 2.0 g/L. The results indicating that the removal efficiencies of As(III) and As(V) increase with increasing IOCS dosage. Moreover, these studies found the As(V) can adsorbed onto IOCS surface better than As(III). The study the effect of pH (6, 7 and 8) on As (III) and As(V) adsorption onto IOCS. The results show that the removal of As(III) and As(V) decreases with increasing pH value. Not only the pH of the As solution that effect to As adsorption capacity onto IOCS, but also has the effect of increasing silica concentration at pH 7 and 8 that can effect to the adsorption of As onto IOCS as well.

The results of increasing silica concentration of 50 mg/l, the As removal efficiencies decreased by 12% and 15% at pH 7 and 8, respectively. According to these results, it is indicated that the negative effect of silica occurs when increasing pH of As solution.

Mak et al. (2011a) studied the combination of ZVI (Fe^0) and IOCS for removal of co-present Cr(VI) and As(V) from groundwater and to estimate the effect of humic acid (HA) to the removal of Cr(VI) and As(V) by using batch experiment. The results found that the mixing of ZVI and IOCS can increased the removal capacity of Cr(VI) and As(V) compared with used of IOCS alone or ZVI alone.

Mak et al. (2011b) studied the removal Cr(VI) and As(V) from groundwater and the effect of HA to the Cr(VI) and As(V) sorption on mixing of ZVI and IOCS by using column experiment. The thirteen columns will pack with different reactive materials consisted of sand, IOCS and ZVI in the single column and duplicate column. The synthetic groundwater consisted of 0.8 mM $CaCl_2$, 3mM HCO_3^-, 1 mM Na_2SO_4, 5 mM NaCl, 20 mg/L Cr(VI), and 10 mg/L As(V) with/without 8 mg/L of HA and the pH of solution was fixed to 7. The synthetic groundwater was flush into the columns via piston pump in an up flow system. The synthetic As(V) solution was flush into the column with the effective velocity about 27.4 cm/day and a flow rate was about 0.1 ml/min. This velocity was referring to the seepage velocity at the Vapokon site, Denmark where installing PRB in this site (Lai et al., 2006). The desired time for one pore volume (PV) was about 17.6-17.7 hours. Groundwater samples were collected every 5 PVs from the sampling ports of the columns and the pH of solution was

measured in every samples. The concentration of Cr(VI) and As(V) and the redox potential will measured by ICP-MS and a flow cell.

As a results, the duplicate column (mixing of an Fe^0 and IOCS) can increase the highest removal capacity of both Cr(VI) and As(V). Moreover, the effect of HA found a little effect on Cr(VI) and As(V) adsorption onto these reactive materials. The results of solid phase analysis found the presence of magnetite (Fe_3O_4) on surface of column that mixing of ZVI and IOCS. The Fe_3O_4 occurs from the product (Fe^{2+}) from the oxidation of ZVI (Fe^0) can be adsorbed onto the IOCS and transform to the magnetite (Fe_3O_4). These iron corrosion product will increased the reactive surface area for Cr(VI) and As(V) and reducing the passivation on the Fe^0. HA can be adsorbed onto the IOCS result in reduced the HA deposition aggregates on the Fe^0 surface and enhancing the Fe^0 corrosion.

Rahman et al. (2013) studied decontamination of spent IOCS from filters used in As(V) removal. In batch experiment, the IOCS dosage was 20 g/L and the initial As(V) concentration was 0.75 mg/L. Thirunavukkarasu et al (2003) observed a maximum removal of As(V) in the pH range of 5–8. Thus, the pH was controlled at 7 in experiments. The modification in the residual As(V) concentration with contact time showed mechanism absorption of As(V) on to IOCS was equilibrium adsorption. The initial As(V) adsorption rate was higher followed by a slower rate and approached an equilibrium adsorption. The results indicated that in the initial time As(V) adsorption rate was rapid after that the As(V) adsorption rate tended to be slowed down because

of the adsorption site was saturated with As(V) adsorbed on the surface. The batch experiment was observed that the concentration of As(V) decreased with time up to 240 minutes and approaching to equilibrium within 360 minutes. It is observed that about 75% of As(V) was adsorbed by IOCS within the first 15 minutes. The As(V) concentration in the adsorbent phase was estimated to be 0.037 mgAs(V)/g during the 6 hours adsorption period.

CHAPTER III

MATERIALS AND METHODS

3.1 Material preparation

Background stock solution was prepared by dissolving sodium nitrate mixed with sodium acetate in DI water and controlling ionic strength at about 0.02 mM. The solution was then adjusted with 0.01 HNO_3^- until the pH values reach 4 and 7 ($\pm$0.2). Individual As(V) stock solutions (10 mg/L) were prepared by dissolving appropriate amount of sodium hydrogen arsenate ($HAsNa_2O_4 \cdot 7H_2O$) in the background solution at pH 4 and 7. Sand, Iron oxide-coated sand (IOCS) and zero-valent iron coated sand combination (ZVICS) with iron oxide-coated sand (IOCS) were used as reactive materials. The surface morphology and the chemical composition on the surfaces of sand, Iron oxide-coated sand (IOCS) and zero-valent iron coated sand (ZVICS) were analyzed by Scanning electron microscopy (SEM) and X-ray diffraction spectroscopy (XRD). The As(V) concentration was measured by Inductively coupled plasma mass spectrometry (ICP-MS).

3.1.1 Sand preparation

To prepare sand for packing column, it was cleaned before use by the procedure described by Zhou et al. (2011) as shown in Figure 3.1.
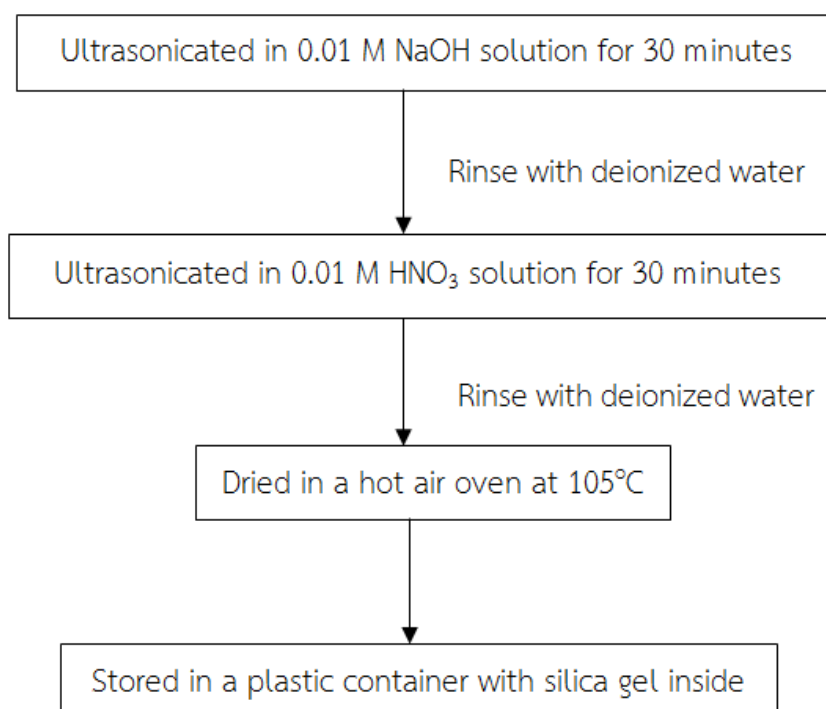
Figure 3.1- Procedure for cleansing the sand before use in the column experiment

3.1.2 Preparation of iron oxide coated sand (IOCS)

The procedure for IOCS described by Dhagat et al. (2013), was show in Figure 3.2.
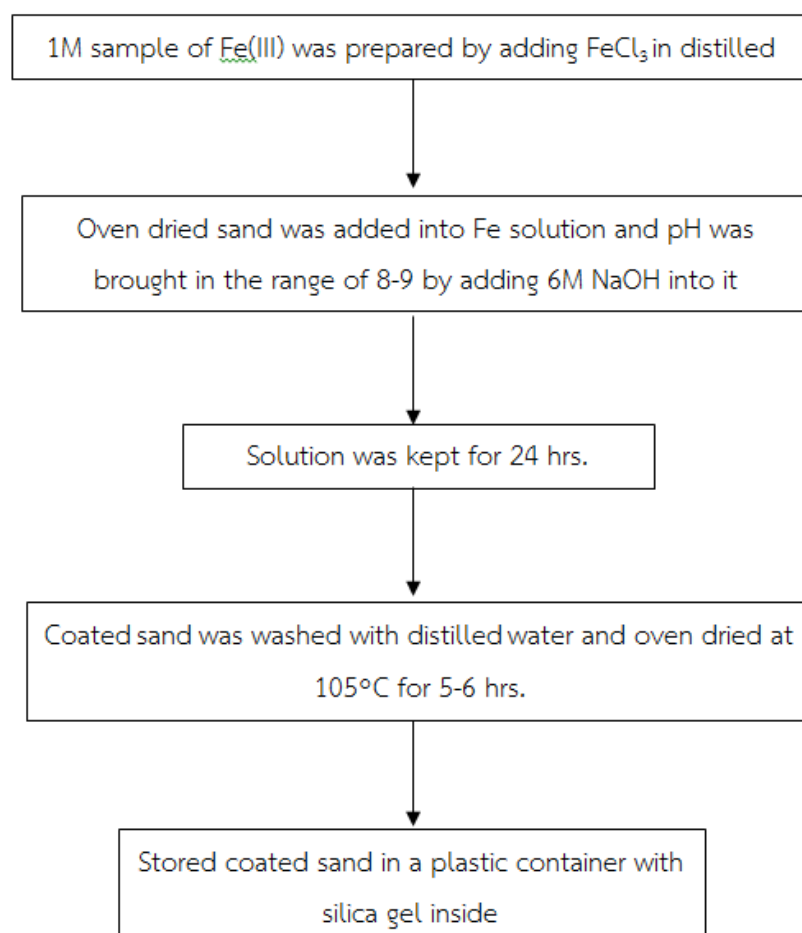
Figure 3.2-Procedure for iron oxide coated sand (IOCS) before use in the column experiment

3.1.3 Preparation of zero-valent iron coated sand (ZVICS)

The following is the method for preparation of zero-valent iron coated sand modified from (Lee & Jou, 2013) and (Uzum et al., 2008) as shown in Figure 3.3.

The zero-valent iron particles were synthesized by drop wise 0.75 M of $NaBH_4$ (about 40-50 drops/min) into 0.135M $FeCl_3 \cdot 6H_2O$ in water bath until pH was 6

The $NaBH_4$ was reduced ferric iron (Fe^{3+}) to zero-valent iron (Fe^0). The reaction occurs as below:

$$4Fe^{3+} + 3BH_4^- + 9H_2O \rightarrow 4Fe^0 + 3H_2BO_3^- + 12H^+ + 6H_2$$

The washed sand particles were submerged in $FeCl_3 \cdot 6H_2O$ solution

The mixer was shaken in water bath at 200 rpm for 4 hours while the temperature was maintained at 60°C.

The solid was washed at least three time with 99% absolute ethanol and purged with N_2 gas to prevent oxidation.

Stored ZVI coated sand in a dark plastic container and kept in dessicator

Figure 3.3-Procedure for ZVICS before using in the column experiment

3.2 Column experiments

3.2.1 Column set up

An acrylic column was 2.5 cm in inner diameter and 10 cm in length. The column was cleansed by 0.01 M NaOH and 0.01 M HNO_3 before doing experiments. After that, the column was packed with sand purchased by FISHER (particle size about 20-30 μm). The influent was pumped via piston pump into the bottom end of the column. The influent was flushed through the saturated sand column with an effective porosity of 0.37, bulk density of 1.51 g/cm^3 and influent velocity was set approximately 0.16 cm/min.
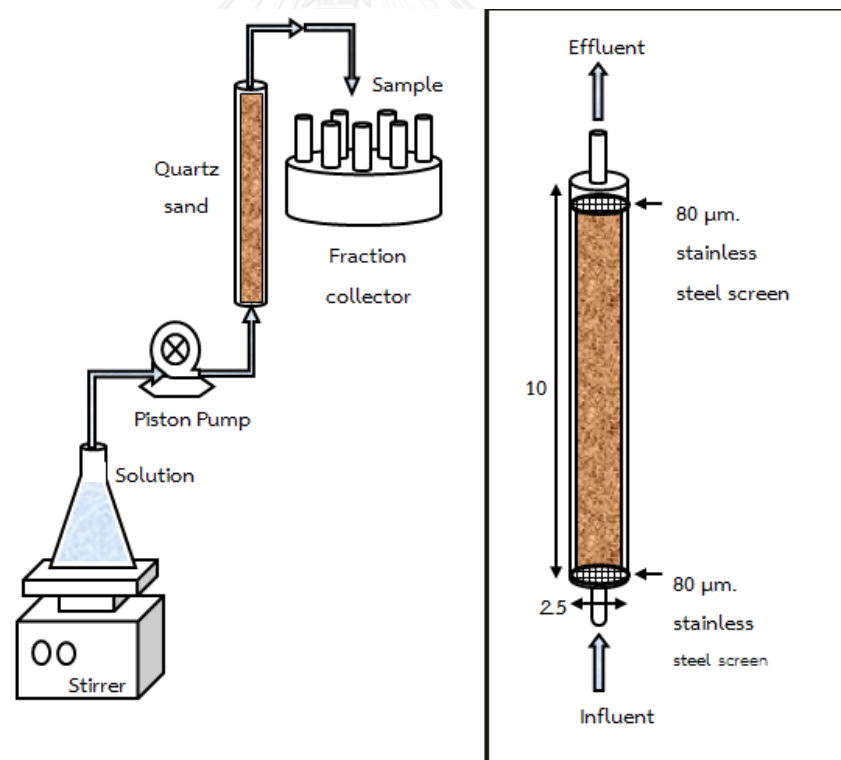
Figure 3.4-Column experiment (Wikiniyadhanee , 2012)

3.2.2 Effect of pH on removal of As(V) in the column experiment

The effect of pH (e.g., 4 and 7) on removal of As(V) in each column was investigated. The goal of this study is to investigate removal of As(V) in combination of IOCS and ZVICS in column experiments compared with IOCS and sand only columns in each pH condition (pH 4 and 7), as shown in Table 3.1 and 3.2.

Table 3.1-Column nos. 1-3 with different reactive materials (Sand, IOCS, ZVICS with IOCS) at pH 4

Column	Reactive materials	Influent solution
1	Sand	As(V) at pH 4
2	Iron oxide coated sand (IOCS)	As(V) at pH 4
3	ZVICS mixed with IOCS (1:1 by mass)	As(V) at pH 4

Table 3.2-Column nos. 1-3 with different reactive materials (Sand, IOCS, ZVICS with IOCS) at pH 7

Column	Reactive materials	Influent solution
1	Sand	As(V) at pH 7
2	Iron oxide coated sand (IOCS)	As(V) at pH 7
3	ZVICS mixed with IOCS (1:1 by mass)	As(V) at pH 7

Steps in conducting of As(V) transport in column experiments as shown below in (Figure 3.5):

1. Before to use packed column for testing As(V) removal, the columns were equilibrated by flushing several pore volumes (PVs) of DI water. Moreover, at least 3-4 PVs of the As(V)-free background solution with a fixed pH value of about 4.0 (±0.2) and

7.0 (±0.2) will be used to flush into the column in order to establish steady state flow and standardize the chemical conditions.

2. The As(V) solutions with different pH conditions (4 and 7) were then pumped to the bottom end of the column via piston pump at a constant velocity about 0.16 cm/min until reaching the plateau.

3. Several PVs of background solution with the same pH condition were applied into the column to make sure that there has no As(V) in the effluent.

4. The effluent was collected in tubes by using fraction collectors at regular time intervals.

5. The As(V) concentration was measured by inductively coupled plasma mass spectrometry (ICP-MS).

6. The breakthrough curves (BTC) of As(V) were represented as the relative pore volume (V_i/V_0) and concentration of As(V) (C_i/C_0).
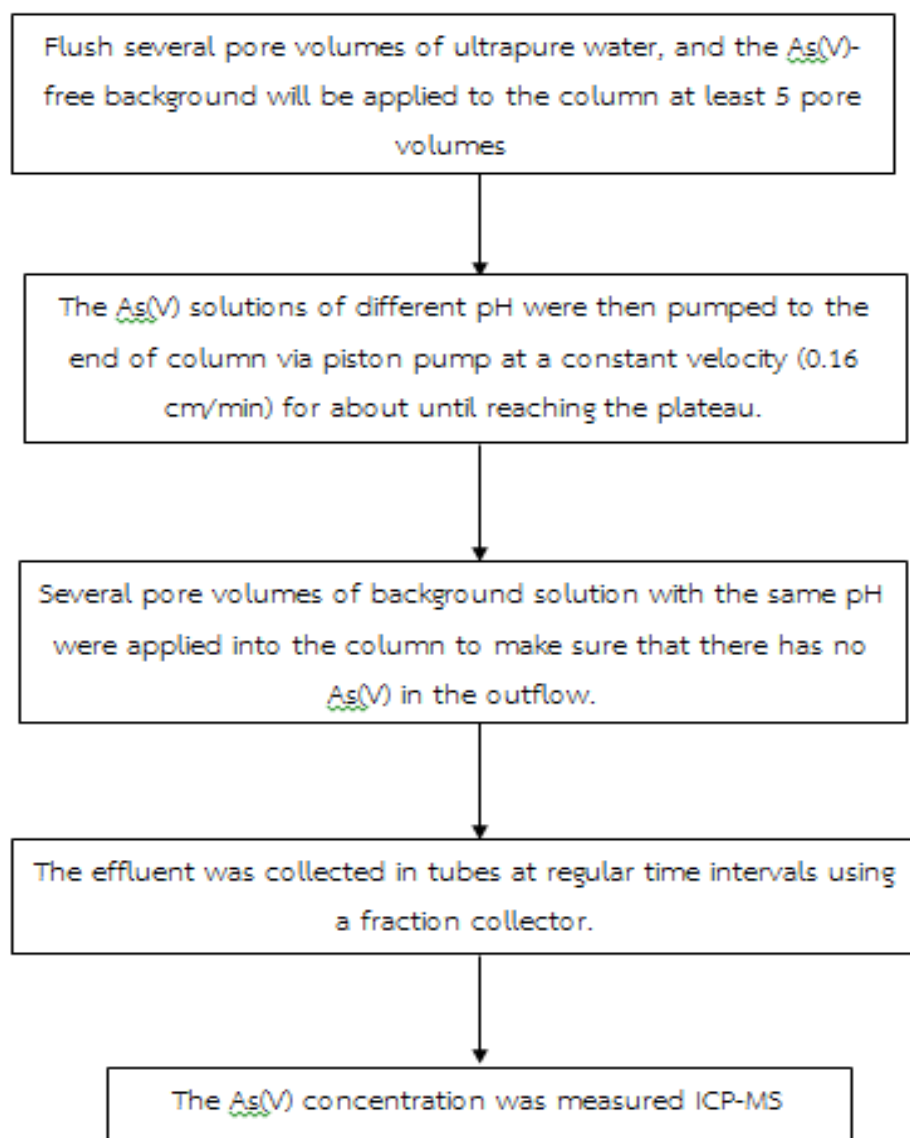
Figure 3.5-Procedure for As(V) transport through column experiment with different material medias and pH conditions

3.3 Microwave digestion

After finishing the transport of As(V) with different pH (4 and 7) in each column, the reacted column fillings (Sand, IOCs and ZVICS combination with IOCS) were

separated into 10 parts, then oven dried at 105°C. Then, the reactive materials were

digested with microwave digestion system followed by Method 3051A
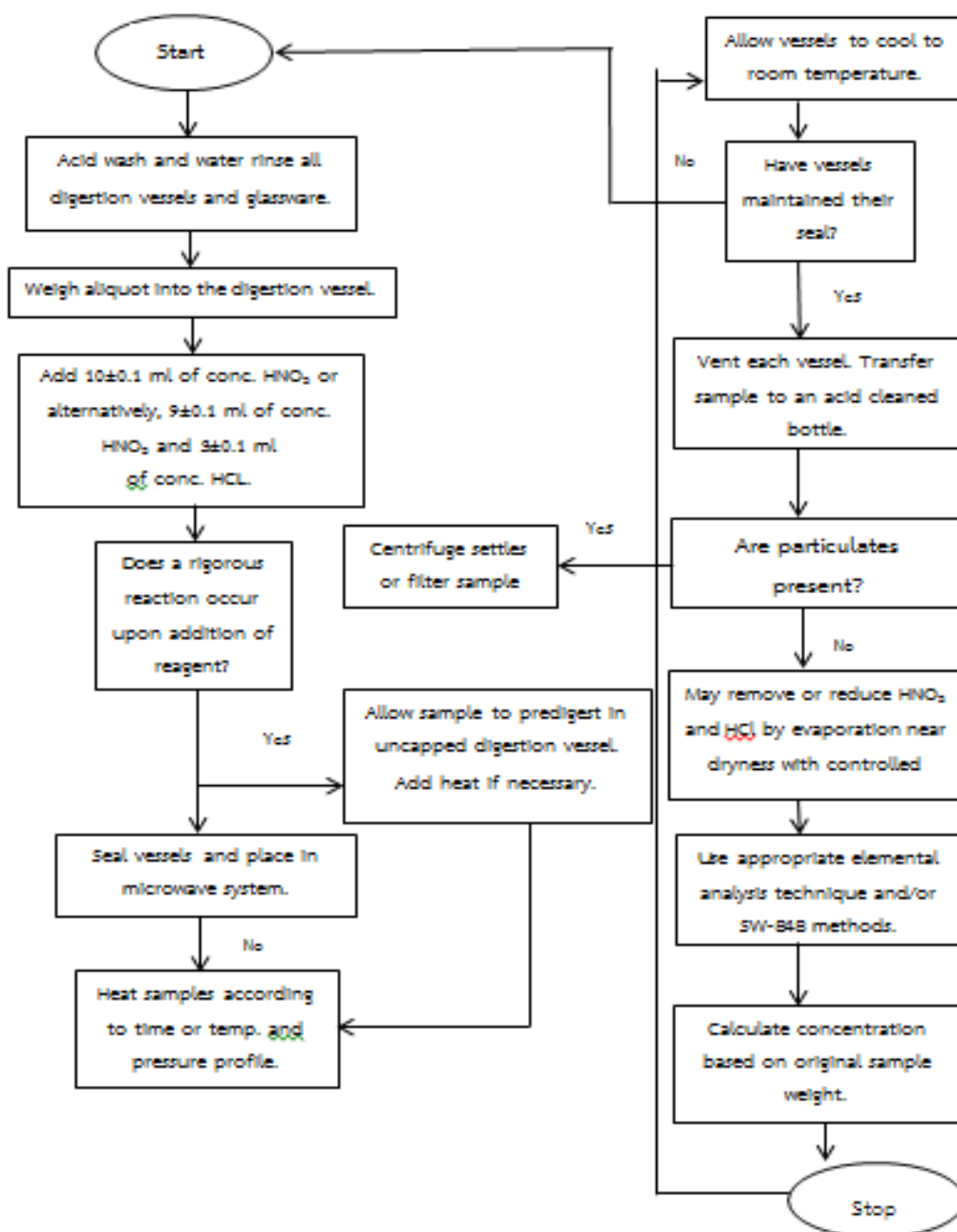
Figure 3.6-Microwave digestion system (Method 3051A)

.4 Analytical methods

The concentration of As(V) was measured by inductively coupled plasma mass spectrometry (ICP-MS).

3.4.1 X-ray spectroscopy analysis(SEM-DEX)

The surface of the reactive materials(Sand,IOCS and ZVICS) were determined by X-ray spectroscopy (SEM-DEX) (Mak et al., 2011) for investigated the different surface of each reactive materials before and after testing As(V) adsorption.

3.4.2 Energy Dispersive X-Ray Spectrometer(EDX/EDS)

The EDX/EDS analysis was performed at randomly selected areas on the solid surface to explain the atomic distribution of the reactive materials surface (Uzum et al., 2008) for make sure As(V) adsorbed onto reactive materials.

3.4.3 X-Ray Diffraction Analysis(XRD)

The material structure of reactive materials(Sand,IOCS and ZVICS) were analyzed by X-Ray Diffraction Analysis(XRD) (Sun et al., 2006), Model D8 Advance: Bruker AXS. The objective of XRD analysis was to explain the different of three reactive materials.

3.4.4 X-ray fluorescence Spectrometry(XRF)

The component of reactive materials were analysis by Wavelength dispersive X-ray fluorescence spectrometry(XRF), Bruker model S8 Tiger.

3.5 Area method

To compare the efficiency of adsorbent were determined by the retardation factors (R_{area}) that calculated by the area method (Nkedi-Kizza et al., 1987). The equation for calculating the retardation factor was shown below:

$$R_{area} = PV_i - \sum_{i=0}^{PV_i} (C/C_0)\, \Delta\, PV$$

Where, C is the concentration of As(V) in the effluent, C_0 is the concentration of As(V) in the influent, and PV_i is the number of pore volume at the relative concentration (C_i/C_0) of As(V) is 1.0.

3.6 Hydrus-1D model

Hydrus-1D model can be used for mimic of water flow and transportation of heavy metal in variably saturated porous media (Simunek & Genuchten, 2008). The model can be applied for different physical equilibrium and chemical non-equilibrium flows and transportation in both direct and inverse models (Chotpantarat et al., 2011).

3.6.1 The uniform (equilibrium) solute transport model

The conceptual of uniform (equilibrium) solute transport model can be expanded in Figure 4.14. In this model, water flow and solute transport occur via pores or fractures between soil particles (or of impermeable soil aggregates or rock fragments). The dissolved solute transport through pores and instantaneously adsorbed onto adsorbent surface.
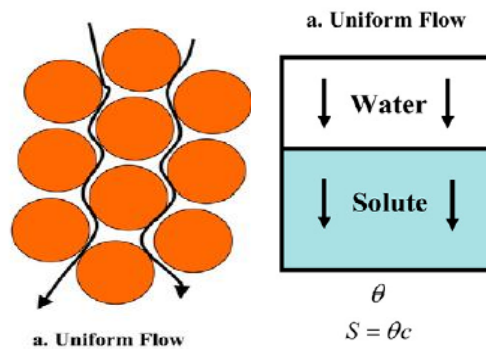
Figure 3.7-Conceptual of uniform (equilibrium) solute transport model (Simunek & Genuchten, 2008).

This study focuses only on solute transport model. The solute transport model is usually described using relative standard advection-dispersion equation (Eq. [1])

$$\frac{\partial \theta c}{\partial t} + \rho \frac{\partial s}{\partial t} = \frac{\partial}{\partial z}\left(\theta D \frac{\partial c}{\partial z}\right) - \frac{\partial qc}{\partial z} - \phi$$

[1]

Where, c is the solution concentration [M·L^{-3}]

s is the sorbed concentration [M·M^{-1}]

D is the dispersion coefficient accounting for both molecular diffusion and hydrodynamic dispersion [L^2·T^{-1}]

q is the volumetric fluid flux density [L·T^{-1}] evaluated using the Darcy–Buckingham law

φ is a sink–source term that accounts for various zero- and first-order or other reactions [M·L^{-3} T^{-1}].

3.6.2 The chemical non-equilibrium two-site model (TSM)

The two-site model is a part of chemical nonequilibrium models. This model can be expanded by supposing the sorption site can be divided in to two fractions (Selim et al. 1976; van Genuchten and Wagenet 1989). One fractions of the sorption site is assumed to be instantaneous, while the second section is assumed to be kinetic sorption. The conceptual of two-site model as shows in Figure 3.8
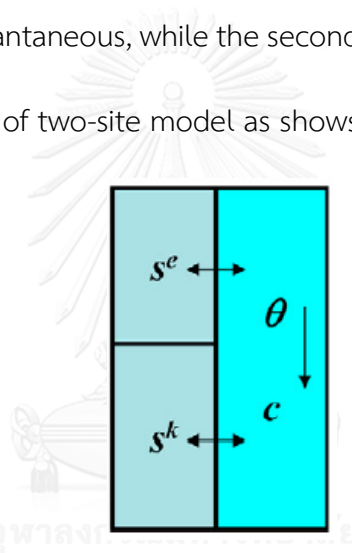
Figure 3.8-Conceptual two-site model for reactive solute transport.

The two-site model (TSM) is considered of nonequilibrium adsorption-desorption reactions. This model can be expanded in term of eq. [2a], [2b], [2c] and [2d]

$$\frac{\partial \theta c}{\partial t} + \rho \frac{\partial s^{e}}{\partial t} + \rho \frac{\partial s^{k}}{\partial t} = \frac{\partial}{\partial z}\left(\theta D \frac{\partial c}{\partial z}\right) - \frac{\partial qc}{\partial z} - \phi$$

[2a]

$$s^{e} = f_{e} K_{d} c$$

[2b]

$$\rho \frac{\partial s^k}{\partial t} = \alpha_k \rho \left(s_c^k - s^k \right) - \phi_k \qquad \text{[2c]}$$

$$s_c^k = \left(1 - f_e \right) K_d c \qquad \text{[2d]}$$

where f_e is the fraction of exchange sites assumed to be in equilibrium with the liquid phase, and α_k is a first-order kinetic rate constant $[T^{-1}]$. c is the solution concentration $[M \cdot L^{-3}]$ Equation [2a] describes solute transport in the total system, Eq. [2b] equilibrium sorption onto the instantaneous sorption sites, Eq. [2c] is a mass balance of the kinetic sorption sites (van Genuchten and Wagenet 1989), while Eq. [2d] represents the sorbed concentration of the kinetic sites when equilibrium would be reached with the liquid-phase concentration.

3.6.3 Parameter estimation

The input parameter required by HYDRUS-1D model were the properties of each column (Sand, IOCS, ZVICS-IOCS) with pH 4 and pH 7 consisted of porosity, bulk density(g/cm^3), seepage velocity(cm/min) were about 0.37, 1.51, 0.1098, respectively. The initial/final As(V) concentration and duration time when start flushing As(V) solution until stop flushing As(V) solution were add to the model.The hydrodynamic dispersion coefficient (D), D=αV, of the saturated sand column was evaluated by curve fitting the bromide BTCs with nonlinear least-squares parameter optimization method of CXTFIT (Toride et.al., 1999). The dispersion coefficient (D) was utilized for calculate in term of advection-dispersion equation of HYDRUS-1D model for estimate sorption parameters of As(V) transport onto saturated sand column under

different pH conditions using linear and nonlinear sorption isotherm model. In addition, the chemical non-equilibrium two-site model with Langmuir sorption ($C_s = K_f \cdot C_l^{(1/n)}$) was used to evaluate the sorption parameter K_d and β from model. The sorption parameter K_d and β represent to K_f and $1/n$ from the Langmuir sorption equation. If β calculated from the model have less value led to the value of K_d have high value. So, when K_d have high value indicated that As(V) preferable adsorbed onto this reactive materials with optimum pH condition. Moreover, the non-equilibrium parameters (f and α) for heavy metal transport shows if the fraction site have a value between 0.90-1.00 the results can assumed that the mechanism of As(V) adsorbed onto reactive materials was equilibrium adsorption. On the contrary, if the fraction site have a value much less than 1.00 the results can assumed that the mechanism of As(V) adsorbed onto reactive materials was non equilibrium two-site model adsorption. Sum of square errors (SSEs) were used to determine the appropriateness of the curve fitting (Chotpantarat et al., 2011).

The results from the column experiment were analyzed by using the Hydrus-1D model (equilibrium model and two-site model) to describe the main mechanisms controlling the As(V) transport in various saturated sand column (i.e.,sand, IOCS, ZVICS-IOCS).

CHAPTER IV
RESULTS AND DISCUSSION

4.1 Chemical properties of Sand, Iron oxide coated sand and zero-valent iron coated sand

Chemical properties of sand, IOCS and ZVICS were elucidated by X-ray fluorescence spectrometry (XRF), Bruker model S8 Tiger. The result of XRF shows that the chemical component of sand consisted of SiO_2; while IOCS and ZVICS consisted of SiO_2 and Fe_2O_3 as major components (Table.4.1). However, the results of XRD pattern were indicated that synthesis reactive materials were IOCS and ZVICS. Moreover, the data of XRD can notice that both of reactive materials (IOCs and ZVICS) are different (Figure. 4.1 and 4.2).

Table 4.1 Physical and chemical properties of original quartz sand, IOCS and ZVICS

Parameter	Quartz sand	Iron oxide coated sand (IOCS)	ZVI-coated sand (ZVICS)
Physical form	Dry pellet	Dry pellet	Dry pellet
Color	White	Dark orange	Dark
Whole grain components (atomic %)	SiO_2 (98) Al_2O_3 (2)	SiO_2(99) Fe_2O_3(0.44) Al_2O_3(0.35)	SiO_2(99) Fe_2O_3(0.52) Al_2O_3(0.22) Na_2O(0.13)
BET area (m^2/g)	n/a	0.78	0.81
pH_{zpc}	5.0±0.03	7.0±0.02	7.5±0.03
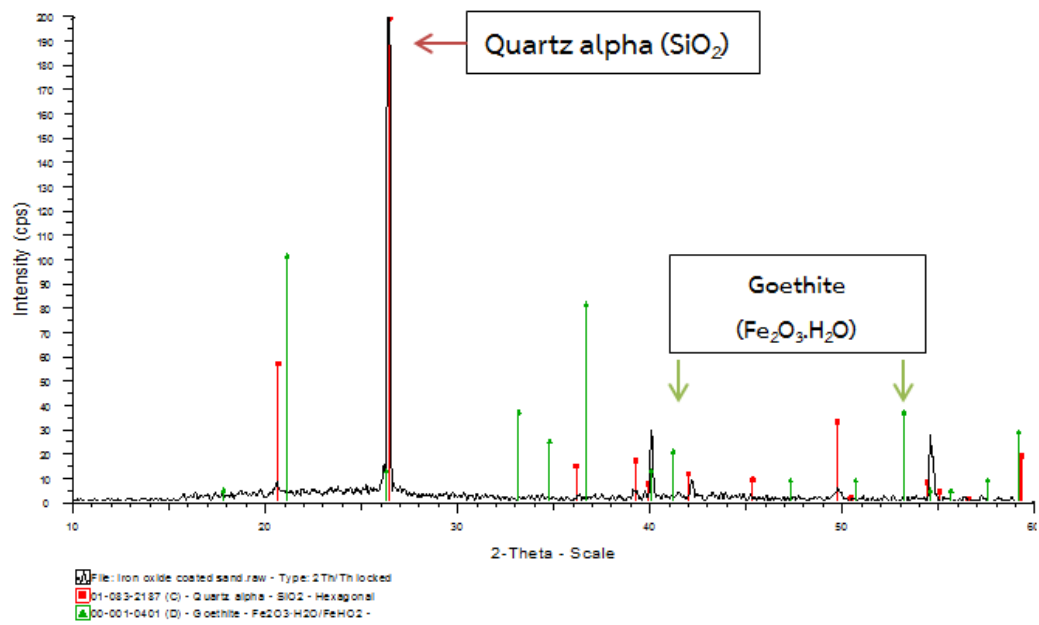
Figure 4.1-X-ray Diffraction pattern of synthesis IOCS
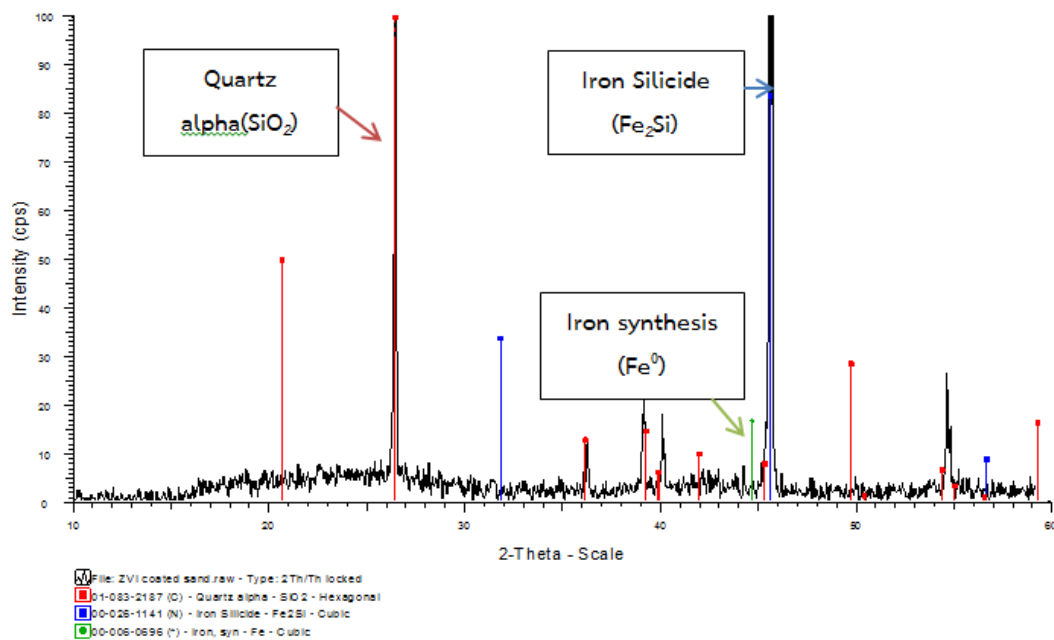
Figure 4.2-X-ray Diffraction pattern of synthesis ZVICS

4.2 Effect of pH (4 and pH 7) on As(V) saturated sand column

As(V) solutions were injected into saturated sand column under different pH 4 and 7 to evaluate the effect of pH to As(V) adsorption. Table 4.2 shows the column properties used in column experiments.

Table 4.2 Column properties of saturated sand for As(V) adsorption under different pH conditions (pH of 4 and 7)

Column	Length (cm)	Diameter (cm)	Bulk density (g/cm³)	Porosity	Seepage velocity (m/day)	pH
Sand	10.00	2.50	1.510	0.377	2.07	4.0±0.1
Sand	10.00	2.50	1.509	0.377	2.07	7.0±0.2

$^{*}R_{area} = 10.17$
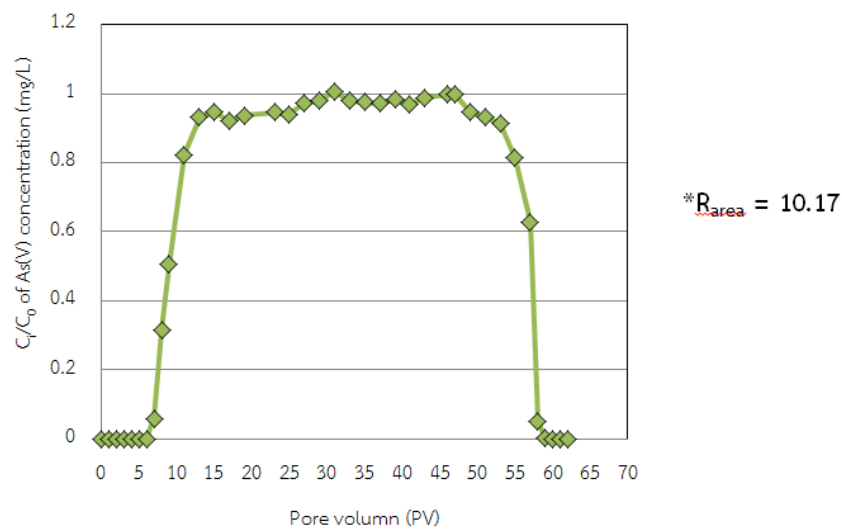
Figure 4.3-Breakthrough curve of As(V) at pH 4 through saturated
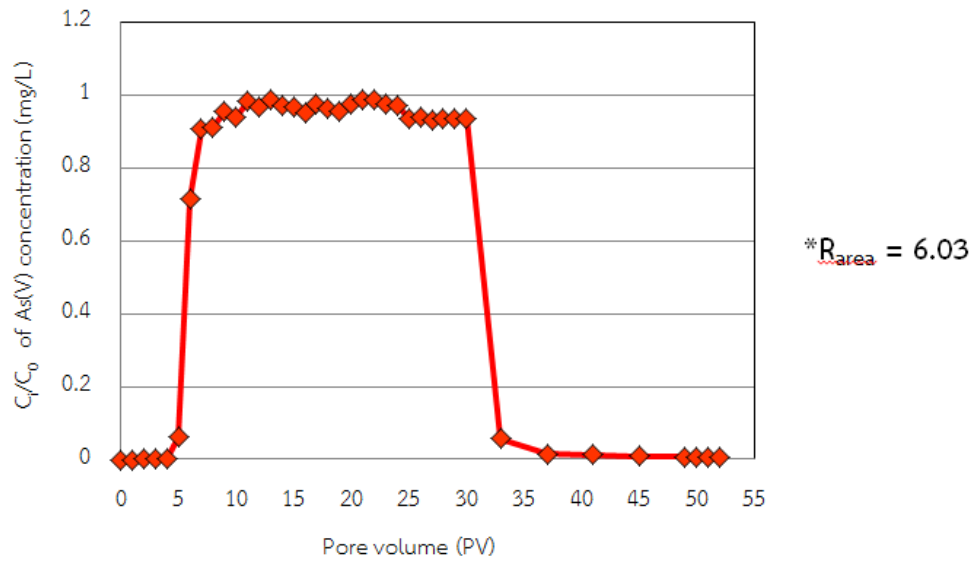
Figure 4.4-Breakthrough curve of As(V) solution with pH 7 through saturated sand column
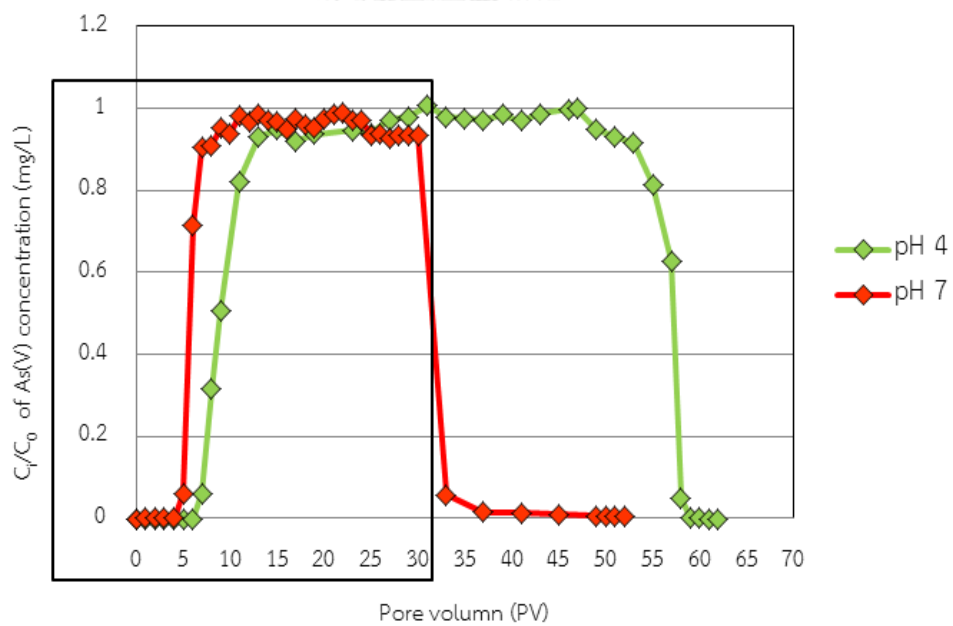
Figure 4.5-Breakthrough curve of As(V) solution with pH 4 and 7 on saturated sand column

Table 4.3 Retardation factor and sorption capacity of As(V) transport through saturated sand column

pH	Initial conc.of As(V) (mg/L)	Retardation factor (R)	As(V)* influent (mg)	As(V) effluent (mg)	%recovery	Sand (g)	Removal capacity (mg As(V)/g)
4	10.71	10.17	8.06	8.02	99.54	74.25	0.0104
7	9.58	6.03	3.99	3.84	96.27	74.13	0.0064

*Calculated from complete breakthrough curve

Figures 4.3 and 4.4 illustrate the effect of solution pH 4 and 7 on saturated As(V) sorption and transport onto saturated sand columns. The breakthrough curves of As(V) transported through saturated sand column in each pH show the maximum relative concentration (C_i/C_0) of As(V) at every solution effluent was 1. However, the time intervals needed for reaching the maximum relative concentration (C_i/C_0) of As(V) in each column were differently. In sand column of pH 4, the maximum relative concentration of (C_i/C_0) As(V) was 1 at 31 PVs while the maximum relative concentration of (C_i/C_0) As(V) was 1 at 11 PVs for the sand column of pH 7.

Table 4.3 gives the information of retardation factor(R) and removal capacity of As(V) transported through saturated sand. The retardation factor (R) and removal capacity of As(V) transport through saturated sand column were decreased from 10.17 to 6.023 and from 0.0104 to 0.0064 mg As(V)/g sand, respectively. The result shows that the As(V) adsorption onto saturated sand was increased with decreasing pH of solution on account of the existence of OH⁻ decrease that could decrease the

competitive adsorption between OH$^-$ and As(V) on the adsorption sites. So, the removal capacity of As(V) onto sand at low pH is higher than at high pH (Genc-Fuhrman et al., 2005). Moreover, from the mass titration curve of quartz sand we found the pH$_{zpc}$ of quartz sand was about 5.0. Therefore, sand surface in column at pH 4 shows positive charge and sand surface column at pH 7 shows the negative charge because when the pH of solution lower than pH$_{zpc}$ the surface charge of sand show positive charge and when the pH of solution higher than pH$_{zpc}$ the surface charge of sand show negative charge. As a result, the adsorption of As(V) in sand column at pH 4 is better than at pH 7 corresponding with retardation factor (R$_{area}$) data. If R$_{area}$ is high value, the adsorption of As(V) onto sand surface is better than less value.

4.3 Effect of solution with pH (4 and 7) onto As(V) sorption onto IOCS column

Table 4.4 Column properties of IOCS for As(V) adsorption under the different pH conditions (4 and 7)

Column	Length (cm)	Diameter (cm)	Bulk density (g/cm^3)	Porosity	Seepage velocity (m/day)	pH
IOCS	10.00	2.50	1.518	0.371	2.07	4.0±0.1
IOCS	10.00	2.50	1.529	0.371	2.07	7.0±0.2
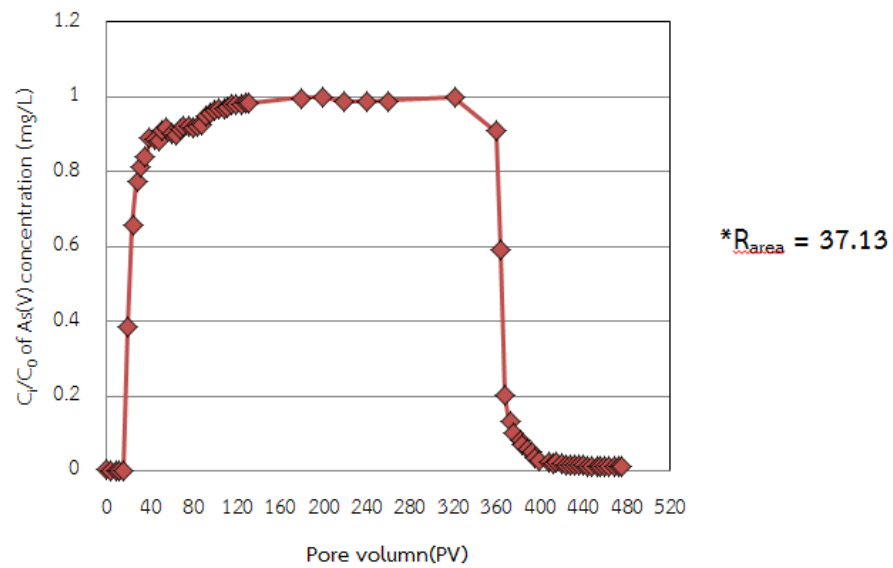
Figure 4.6-Breakthrough curve of As(V) at pH 4 through IOCS column
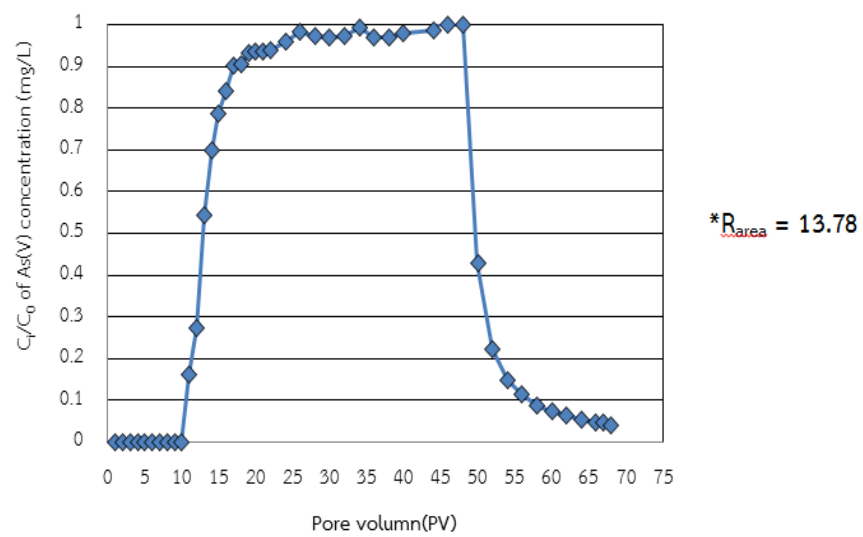
Figure 4.7-Breakthrough curve of As(V) at pH 7 through IOCS column
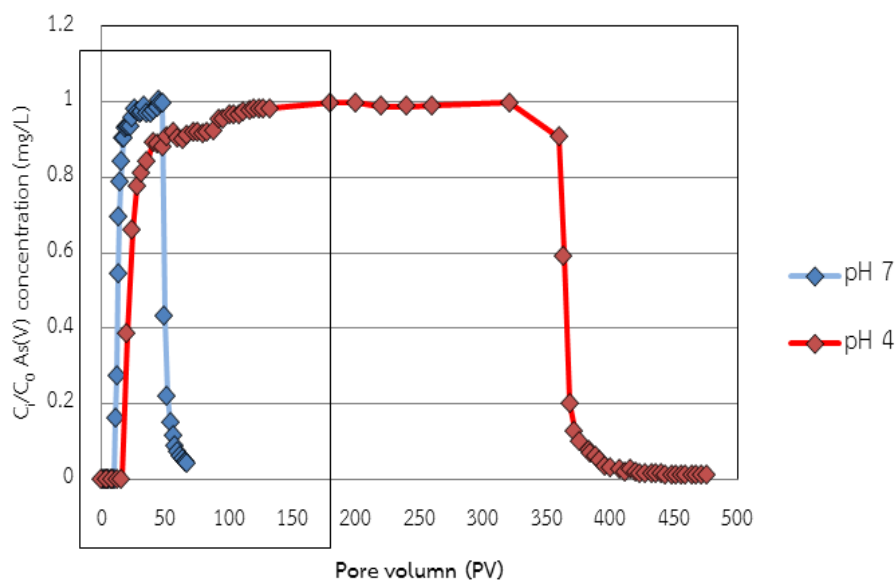
Figure 4.8-Breakthrough curve of As(V) at pH 4 and 7 through IOCS

Table 4.5 Retardation factor and sorption capacity of As(V) transported through IOCS column

pH	Initial conc.of As(V) (mg/L)	Retardation factor (R)	As(V)* influent (mg)	As(V) effluent (mg)	%recovery	Sand (g)	Removal capacity (mg As(V)/g)
4	9.34	37.13	49.76	49.52	96.27	74.57	0.0240
7	8.26	13.78	5.95	5.97	92.01	74.80	0.0115

 * Calculated from complete breakthrough curve

Figures 4.6 and 4.7 demonstrate the effects of As(V) solutions with pH 4 and 7 on IOCS. The breakthrough curves of As(V) transported through iron-oxide coated sand columns shows the maximum relative concentration of (C_i/C_0) As(V) at every solution effluent as 1. However, time interval for reaching the maximum relative concentration of (C_i/C_0) As(V) in each column were different. For IOCS column with pH 4, the maximum relative concentration of (C_i/C_0) As(V) was 1 at 116 PVs while a the maximum

relative concentration of (C_i/C_0) As(V) was 1 at 26 PVs for iron oxide-coated sand column at pH 7.

Table 4.5 shows the retardation factor(R) and removal capacity of As(V) transported through iron-oxide coated sand. The retardation factor and removal capacity of As(V) solutions with pH 4 and pH 7 transported through iron-oxide coated sand column were decreased from 37.13 to 13.78 and 0.0240 to 0.0115 mgAs(V)/g, respectively. Similarly, (Gupta et al., 2005) studies adsorption of As(III) on IOCS in batch studies. The result found the adsorption capacity of the coated sand is higher than the uncoated sand from 0.0285 mg/g to 0.0056 mg/g. According to (Lai et al., 2002) found that coating iron oxide on sand surface will increase the pore site that is available for the heavy metal solute to be adsorbed.

The results illustrate that the As(V) adsorption decreases with increasing pH value concern with the studies (Hsu et al., 2008) the adsorption capacity of As(V) at pH 5, pH 6, pH 7 and pH 8 was 0.022 mg/g, 0.0215 mg/g, 0.021 mg/g and 0.0175 mg/g, respectively. The removal capacity results from column experiment at column pH 4 and pH 7 wasn't nearly the adsorption capacity from Hsu et al. 2008 may be because of the different approach result in the different sorption capacity. Moreover, the results of mass titration curve show pH_{zpc} of IOCs was about 7.0. Thus, when the pH of solution is less than 7, the IOCS's surface charge shows positive charge. On the contrary, if the pH of solution pH equal to pH_{zpc} of IOCS (pzc of IOCS was 7), the IOCS's surface is neutral charged. As a result, positive charge of IOCS may increase the removal of AsO_4^{3-}

, $HAsO_3^{2-}$, $H_2AsO_4^-$ and AsO_2^- through adsorption (Hsu et al., 2008). Furthermore, the R_{area} value of IOCS column at pH 4 was 37.13 higher than IOCS column at pH 7 was 13.78. So, the removal of As(V) in IOCS column at 4 was better than that of pH 7.

4.4 Effect of solution pH (4 and 7) on As(V) sorption onto IOCS-ZVICS combination column

Table 4.6 Column properties of IOCS combination with ZVICS for As(V) adsorption under different condition (4 and 7)

Column	Length (cm)	Diameter (cm)	Bulk density (g/cm³)	Porosity	Seepage velocity (m/day)	pH
IOCS+ZVICS	10.00	2.50	1.5235	0.3658	2.07	4.0±0.1
IOCS+ZVICS	10.00	2.50	1.5234	0.3659	2.07	7.0±0.3
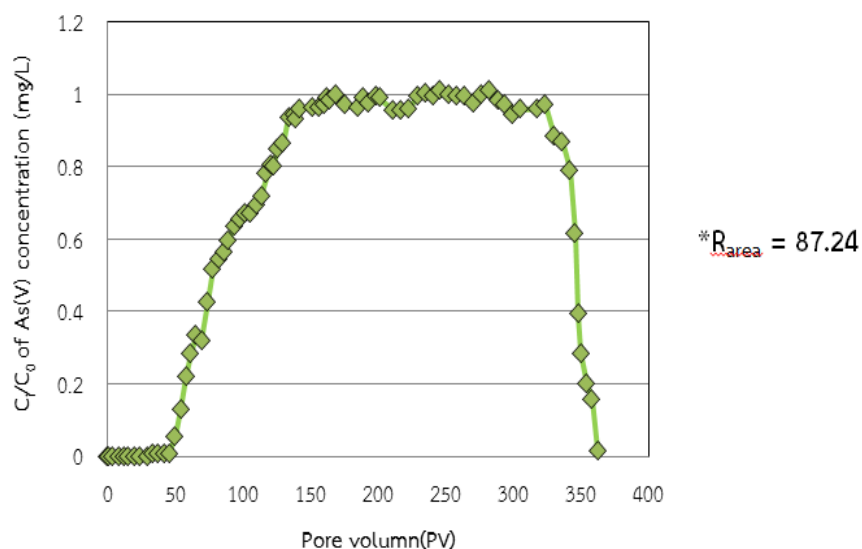
Figure 4.9-Breakthrough curve of As(V) at pH 4 through combination of IOCS and ZVICS column
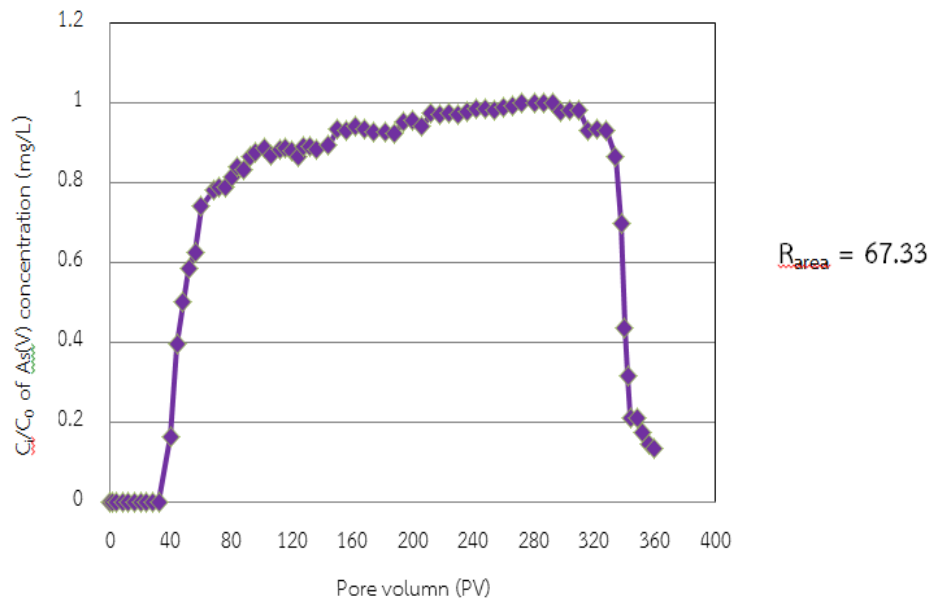
Figure 4.10-Breakthrough curve of As(V) at pH 7 through combination of IOCS and ZVICS column
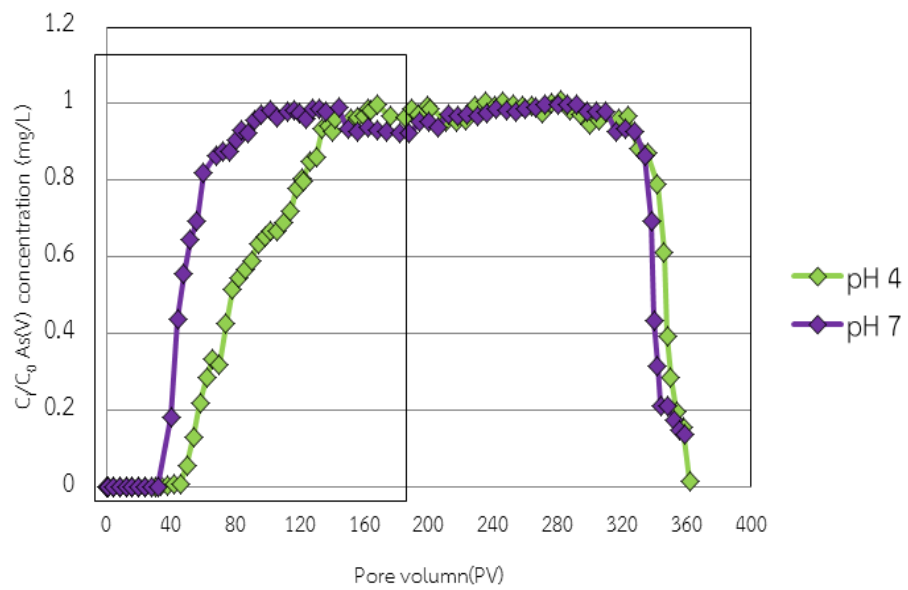
Figure 4.11-Breakthrough curve of As(V) at pH 4 and pH 7 through combination of IOCS and ZVICS columns

Table 4.7 Retardation factor(R) and sorption capacity of As(V) transported through combination of IOCS-ZVICS columns

pH	Initial conc.of As(V) (mg/L)	Retardation factor (R)	As(V)* influent (mg)	As(V) effluent (mg)	%recovery	Sand (g)	Removal capacity (mg/g)
4	9.73	87.24	85.75	84.80	90.29	74.80	0.0328
7	8.77	67.33	51.06	43.05	84.31	74.79	0.0135

* Calculated from complete breakthrough curve

Figures 4.9 and 4.10 show the effects of As(V) solution with pH 4 and pH 7 on ZVI coated sand and IOCS combination column. The breakthrough curves of As(V) transported through ZVI coated sand and IOCS combination column shows the maximum relative concentration of (C_i/C_0) As(V) at every solution effluent of 1. However, the time intervals for reaching the maximum relative concentration of (C_i/C_0) As(V) in each column were different. In the ZVI coated sand and IOCS combination column of pH 4, the maximum relative concentration of As(V) (C_i/C_0) was 1 at 142 PV; and the ZVI coated sand and IOCS combination column with pH 7, the maximum relative concentration of (C_i/C_0) As(V) was 1 at 96 PVs for the IOCS-ZVICS combination column of pH 7.

The results (Table 4.7) show the retardation factor(R) and sorption capacity of As(V) transported through ZVI coated sand and IOCS combination column. The retardation factor (R) and sorption capacity of As(V) at pH 4 and pH 7, transported through IOCS and ZVI coated sand combination columns were decreased from 87.24

to 67.33 and removal capacity were decreased from 0.0328 to 0.0135 mg As(V)/g, respectively.

The results showed the As(V) removal decrease with increasing pH which is similar to the resulting phenomenal of sand and IOCS column. In addition, the results of R_{area} and removal capacity (mg/g) of ZVICS combine with IOCS better than those of IOCS and sand columns ($Q_{zvocs-iocs} > Q_{iocs} > Q_{sand}$). It can conclude that the mixing of ZVI coated sand and IOCS can increase the removal capacity of As(V) compared with using IOCS only and sand only packed in columns. The retardation factor and removal capacity can be summarized below:

At pH 4

R_{sand} (10.17) < R_{IOCS} (37.13) < $R_{ZVICS-IOCS}$ (87.24)

Q_{sand} (0.0104) < Q_{IOCS} (0.0240) < $Q_{ZVICS-IOCS}$ (0.0328)

At pH 7

R_{sand} (6.03) < R_{IOCS} (13.78) < $R_{ZVICS-IOCS}$ (67.33)

Q_{sand} (0.0064) < Q_{IOCS} (0.0115) < $Q_{ZVICS-IOCS}$ (0.0135)

The results of pH_{zpc} value of ZVI coated sand combination with iron oxide coated sand (IOCS), IOCS and sand was 7.5, 7.0 and 5, respectively. The higher pH_{zpc} value result in the more negatively charge on the adsorption area. As a result, the adsorption of As(V) onto mixing of ZVI coated sand and IOCS was better than those of IOCS and sand columns.

In conclusion, As(V) adsorption onto different reactive materials under acidic and neutral conditions were carried out. It was observed that As(V) removal increase with decreasing pH value. Moreover, pH_{zpc} value from the mass titration curve of each reactive material has higher than pH of As(V) solution lead to the surface charge of 3 reactive materials (ZVICS-IOCS, IOCS and sand) shows a positive charge under acidic and neutral condition. The opposite charge between adsorbate and adsorbent will enhance As(V) removal through electrostatic adsorption (Tanboonchuy et al., 2011).

4.5 SEM analysis

The SEM image was used to determine the surfaces of the reactive materials. The EDX/EDS analysis was used to explain the atomic distribution on the surfaces of the reactive materials.
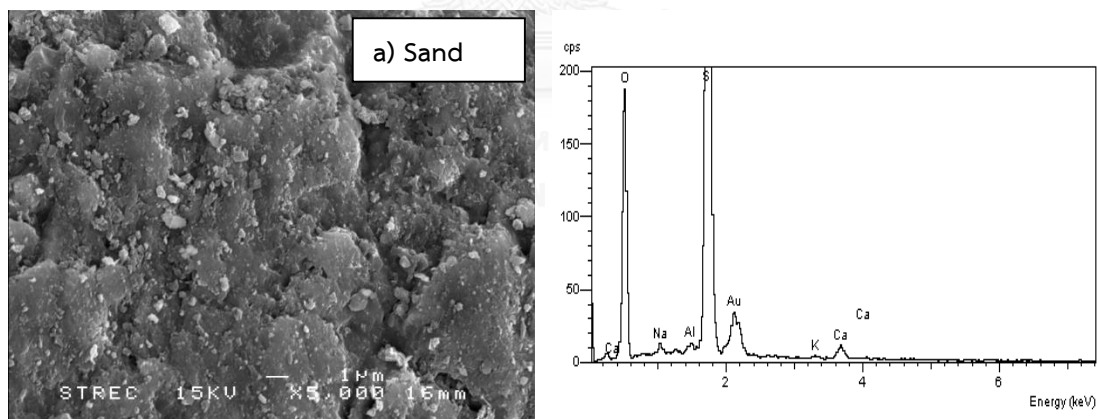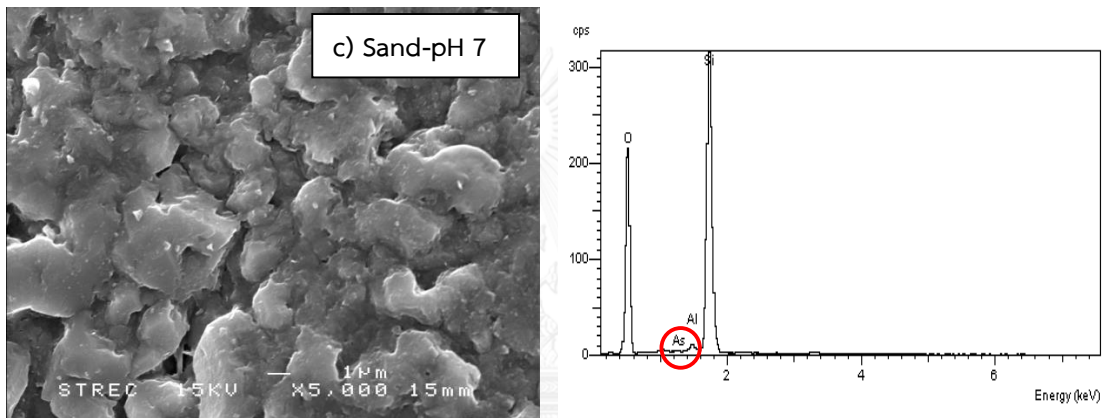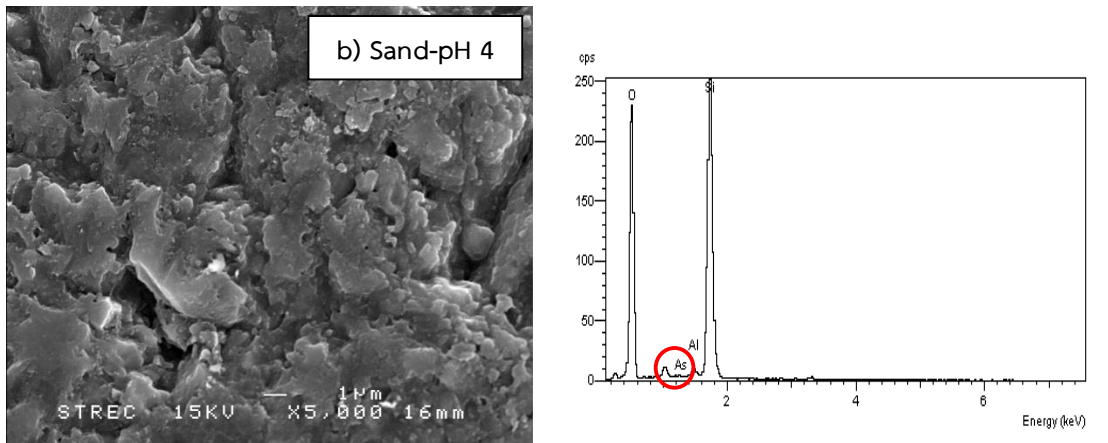
Figure 4.12-SEM images and the corresponding EDX spectrum of the quartz sand (a), quartz sand at pH 4 (b) and pH 7 (c) collect form column
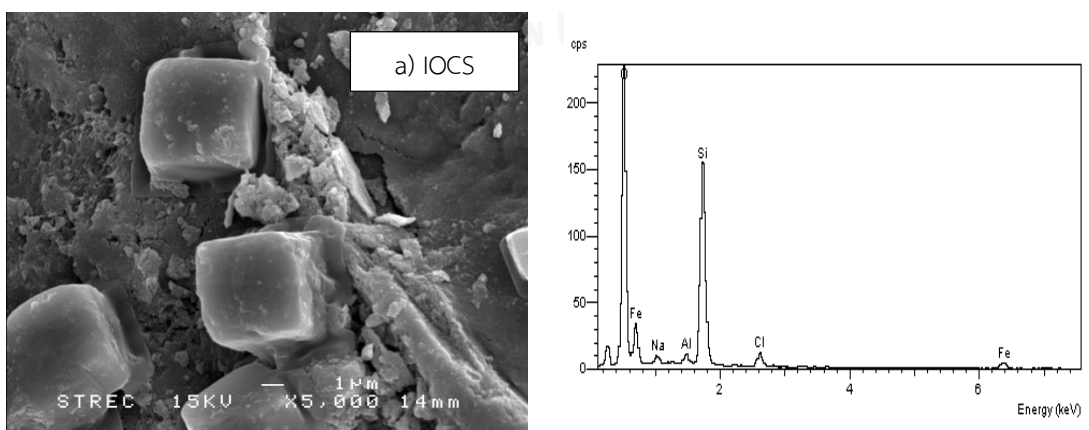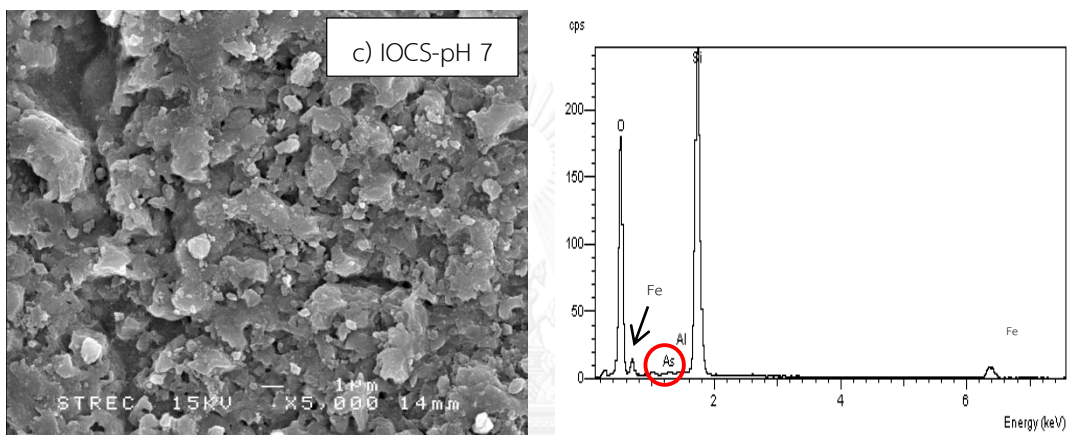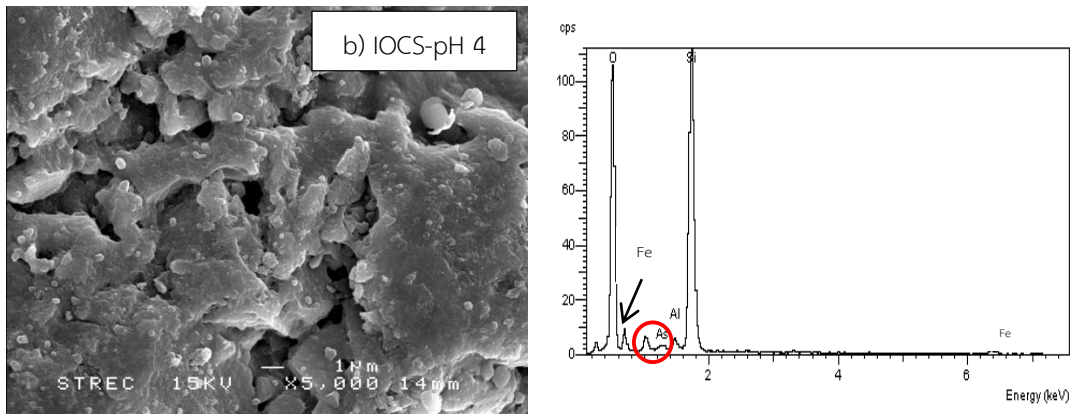
Figure 4.13-SEM images and the corresponding EDX spectrum of the IOCS (a), IOCS at pH 4 (b) and pH 7 (c) collect form column
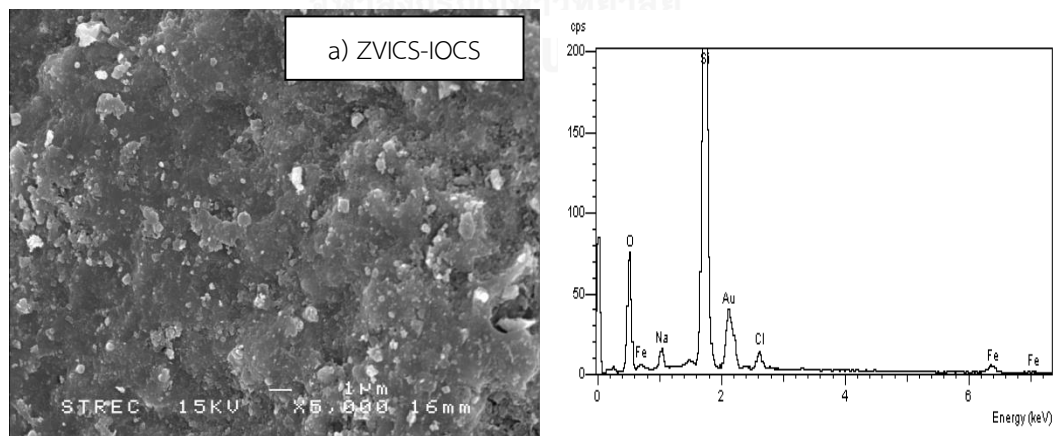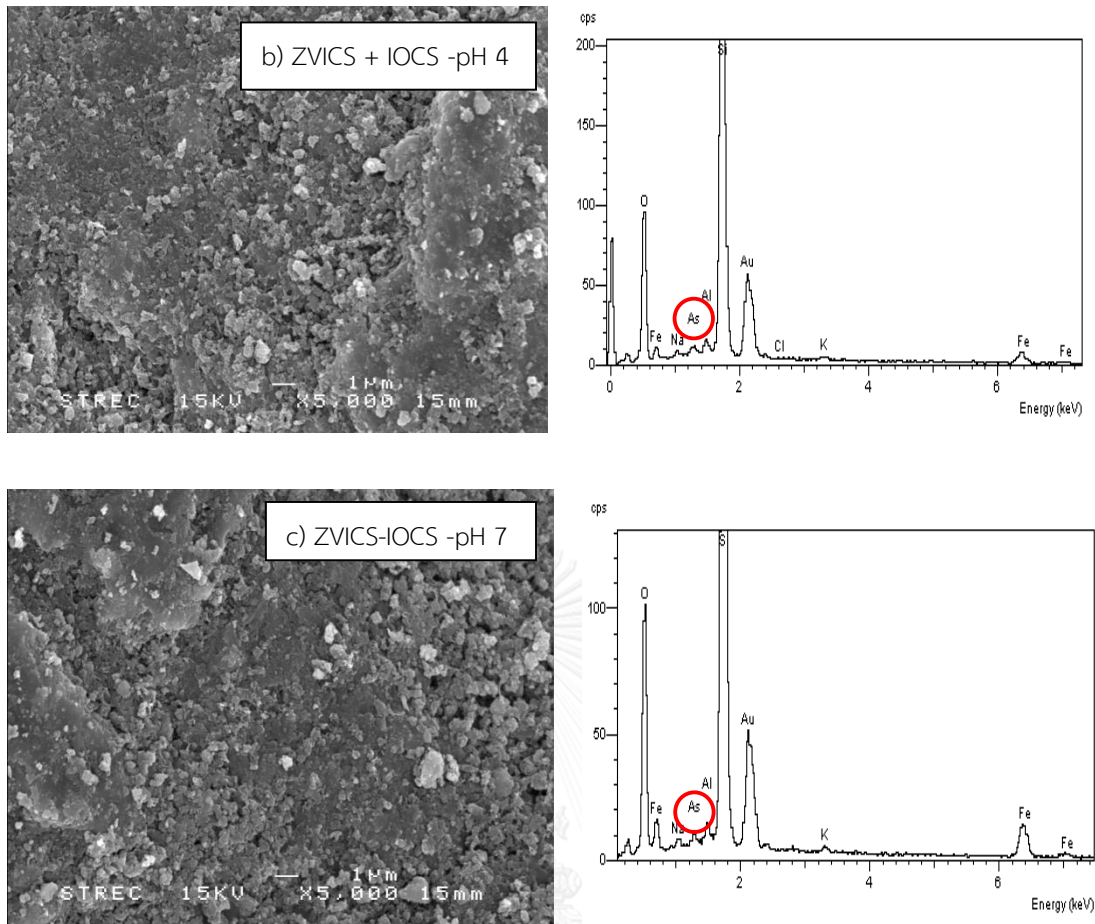
Figure 4.14-SEM images and the corresponding EDX spectrum of the ZVICS-IOCS (a), ZVICS-IOCS at pH 4 (b) and pH 7 (c) collect form column

The SEM images and the corresponding EDX spectrum of acid-washed natural sand, IOCS and ZVICS with IOCS before and after finished As(V) transport through columns at differents conditions were shown in Figure 4.12-4.14

Figure 4.12(a) shows roughness surface of natural sand gains; while, The surface of sand after finished transport test at pH 4 and pH 7 as shown in Figure 4.12(b) and 4.12(c), respectively. The result shows surface of sand after finished As(V) transport test at pH 4 and 7 has a different surface from natural sand before testing As(V) transport. Moreover, It also notices that the SEM image of sand at pH 4 (Fig. 4.12(b)) has higher

porous media than that at pH 7. As a results, the opportunity to adsorb As(V) onto sand at pH 4 could be more than at pH 7. The result of corresponding EDX spectrum of sand column both of pH 4 and 7 shows peak of As(V). These is the evident to confirm that As(V) adsorbed onto sand.

The surface of IOCS as shows in figure 4.13(a) was observably consisted of tetragonal structures of goethite, which was consistent with the XRD results, displaying crystalline goethite on the surface of IOCS (Lai et al., 2002). On the other hand, they found that the pore size was increased by coating the crystalline goethite on the sand's surface. The specific surface area of IOCS (0.78 m^2/g) is larger than that of uncoated sand. Thus, adsorption of As(V) onto IOCS better than that of sand that corresponding with results of retardation factor of IOCS (Table 4.5).The adsorption mechanism of As(V) on IOCS occur by the Fe(III) oxide coated sand adsorbent are oxidized to FeOOH (hydrous ferric oxide) after that As(V) oxyanions are attracted to IOCS and bound with active site (-OH group). Finally, they are bound with the IOCS surface and eliminate water molecules (Maji et al., 2013). Moreover, SEM image of IOCS after As(V) transport test at pH 4 seemed to be higher micropore than that onto IOCS surface at pH 7, indicating that As(V) adsorption onto IOCS at pH 4 become better than that of pH 7. The EDX spectra were collected from randomly selected point on adsorbent surface. The result of corresponding EDX spectrum shows peak of As(V) both of pH 4 and 7. These is the information that can be verified adsorption of As(V) onto IOCS surface.

From Figure 4.14 shows SEM image of ZVICS and IOCS combination collected column from at pH 4 and 7, with some observable likely secondary corrosion products which has characteristic resemble boulder-like precipitate. The corrosion product, Fe^{2+}, was produced from Fe^0 corrosion. It would be adsorbed onto IOCs and transformed to magnetite (Fe_3O_4). The synergistic effect occurred in Fe^0 and IOCs mixture, leading to the higher reactivity of Fe^0, and production of more corrosion products. This is due to the increased reactive surface of As(V). Moreover, the mixture of Fe^0 and IOCS shows the highest removal capacity of As(V) compared to IOCS alone (Mak et al., 2011).

The energy dispersive X-ray (EDX) analysis was used to evaluate the elemental content of the mixing of ZVICS and IOCS column after uptake As(V). The EDX spectra were collected from randomly selected points on adsorbent surface. The result indicated the presence of Fe appearing 3 peaks of energy were about 0.75 keV, 6.40 keV and 7.0 keV. On the contrary, IOCS shows EDX spectrum just 2 peaks of Fe energy about 0.75 keV and 6.40 keV. The studies of (Tanboonchuy et al., 2011) shows that the EDX profile of nano zero-valent iron (nZVI) appear Fe energy peaks at 6.40 keV and 0.75 keV. Therefore, the EDX spectrum of ZVI coated sand combination with IOCS can justify that randomly surface area consisted of iron oxide and zero-valent iron element on sand surface.

4.6 Microwave digestion

*28.14 > *9.17 > *0.49
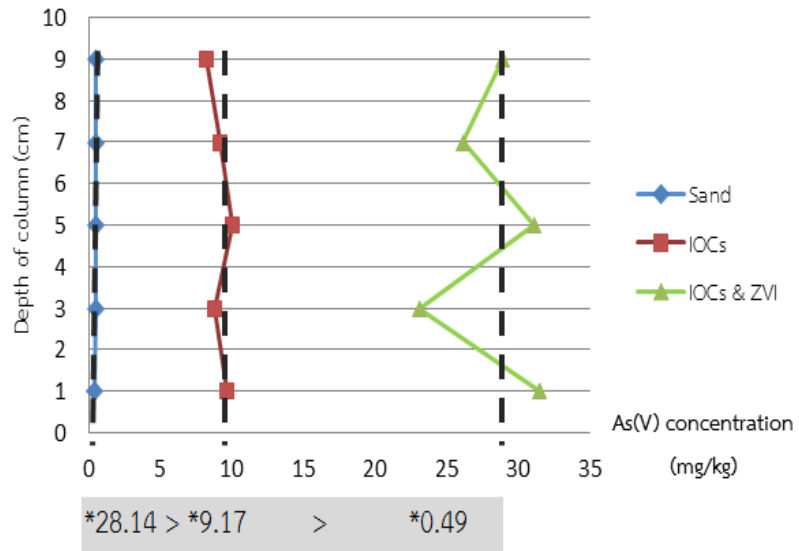
*Average sorption capacity (mg/kg)

Figure 4.15-The adsorption capacity of As(V) onto Sand, IOCs and ZVI coated sand and IOCS combination at pH 4

*19.22 > *4.02 >*0.09
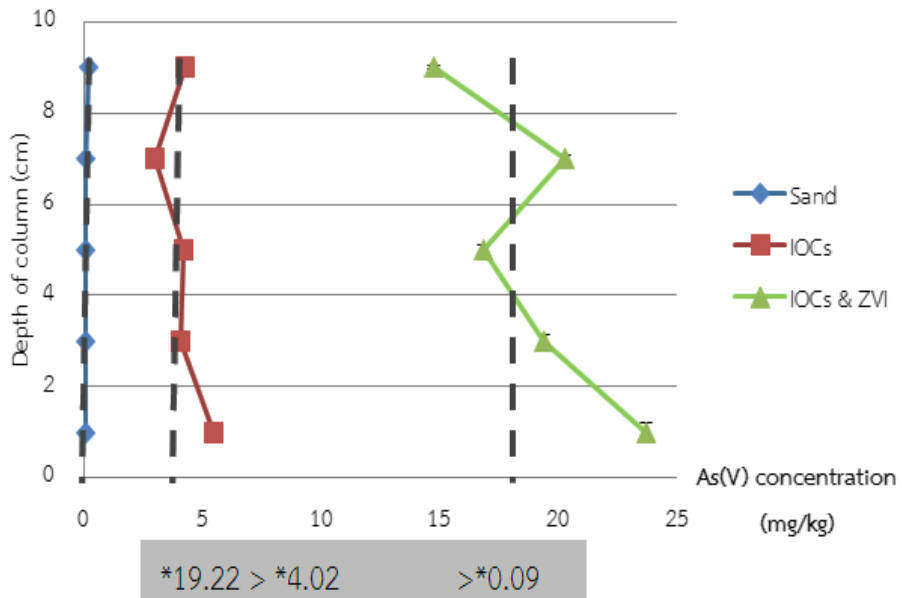
*Average sorption capacity (mg/kg)

Figure 4.16-The adsorption capacity of As(V) onto Sand, IOCs and ZVI coated sand and IOCS combination at pH 7

The As(V) adsorption capacity data from microwave digestion can be explained the main sorption mechanisms, controlling the As(V) transport in saturated sand, IOCs and IOCs combination with ZVICS

Figure 4.15 and 4.16 show that average As(V) sorption capacity (mg/g) of ZVICS-IOCS column at pH 4 and pH 7 were about 28.14 mg/kg and 19.02 mg/kg, IOCS column at pH 4 and 7 were about 9.17 mg/kg and 4.22 mg/kg, Sand at pH 4 and pH 7 were 0.49 mg/kg and 0.09 mg/kg. The results of microwave digestion indicated that the As(V) retained on the mixing of ZVICS-IOCS more than IOCS and sand column. The results of microwave digestion can confirm that the pH of solution affect to As(V) adsorption onto reactive site. Moreover, coating sand with iron oxide and zero-valent iron increase As(V) specific surface area.

Table 4.8 Estimated transport parameters for As(V) breakthrough curves from equilibrium convection-dispersion and non-equilibrium approaches(two-site model) generated by Hydrus-1D model.

Column pH		Equilibrium model fitting				Non- Equilibrium model fitting(TSM)					
		$K_d\pm95\%Cl$	$\beta\pm95\%Cl$	SSE	R_{square}	$K_d\pm95\%Cl$	$\beta\pm95\%Cl$	$\alpha\pm95\%C$	SSE	$f\pm95\%Cl$	R_{square}
1. Sand	pH 4	9.81	0.58	0.6143	0.9763	9.50	0.59	0.0040	0.6210	0.99	0.9758
2. Sand	pH 7	5.57	0.41	0.2506	0.9913	7.20	0.37	0.0038	0.2788	0.09	0.9894
3. IOCS	pH 4	22.70	0.45	0.9256	0.9256	52.21	0.29	0.0006	0.4722	0.55	0.9759
4. IOCS	pH 7	15.59	0.36	0.4255	0.9729	18.00	0.35	0.0050	0.3217	0.90	0.9805
5. IOCS + ZVI coated sand	pH 4	220.00	0.02	0.0622	0.8667	516.00	0.01	0.0003	0.0265	0.01	0.9182
6. IOCS+ ZVIcoated sand	pH 7	57.10	0.14	1.9937	0.9058	108.00	0.21	0.0006	0.4042	0.08	0.9717

*K_d is the distribution coefficient (L^3/M), f the fraction of sorption sites, α is a first-order kinetic rate coefficient and SSE is sum of square error
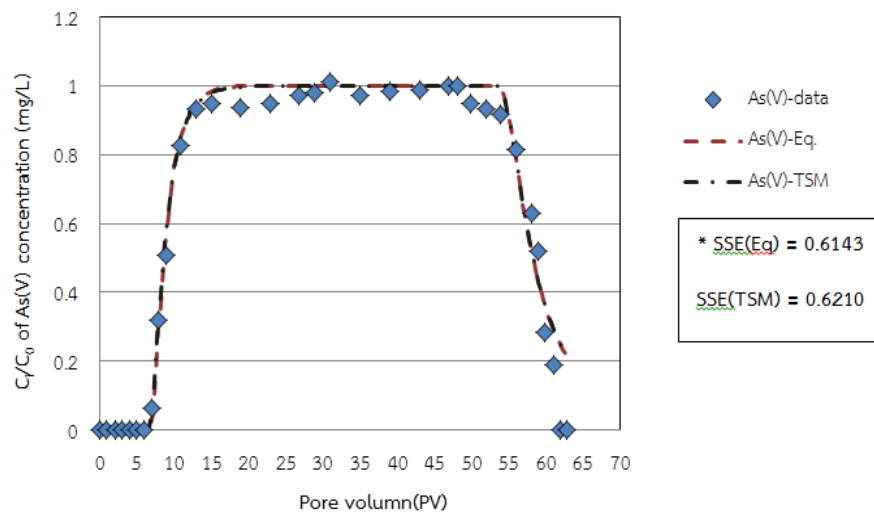
Figure 4.17-As(V) breakthrough curves from saturated sand column experiment at pH 4.0 and As(V) fitted curves with equilibrium model (CDE) and nonequilibrium model (TSM) by using HYDRUS-1D model
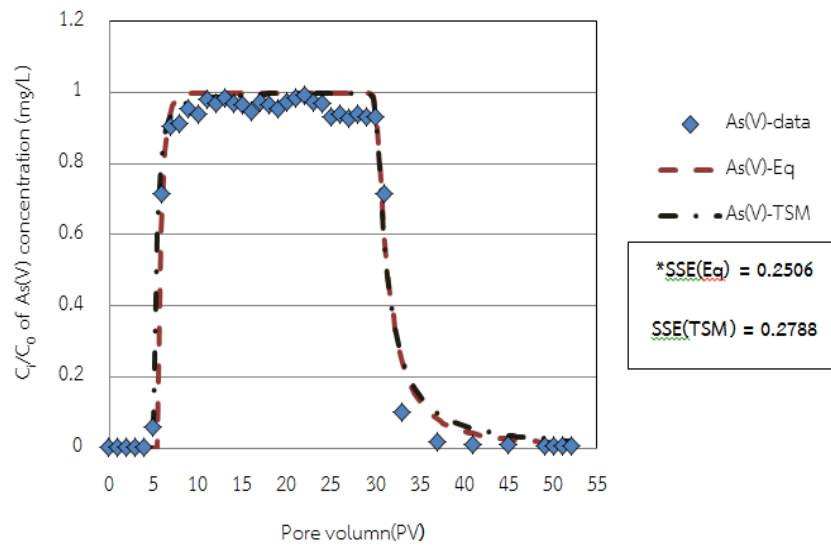
Figure 4.18-As(V) breakthrough curves from saturated sand column experiment at pH 7.0 and As(V) fitted curves with equilibrium model (CDE) and nonequilibrium model (TSM) by using HYDRUS-1D model.
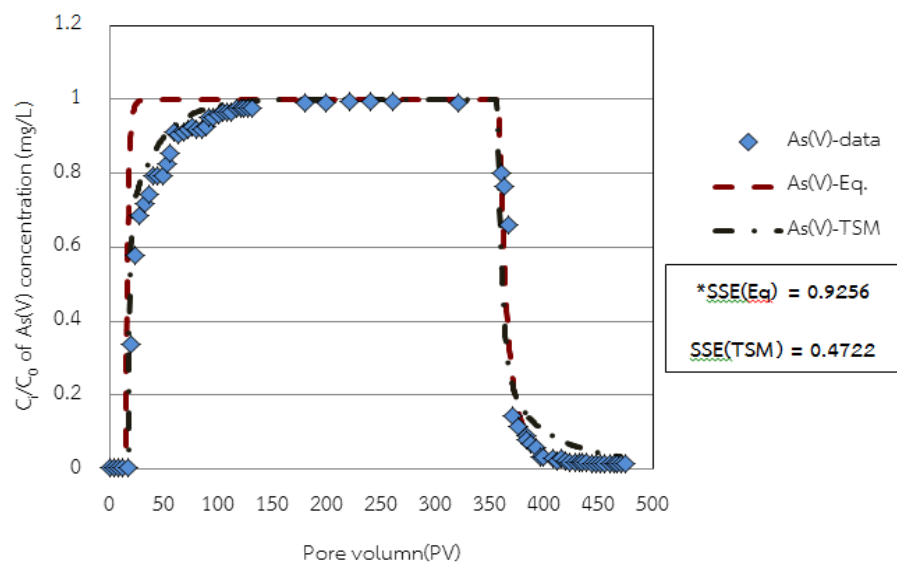
Figure 4.19-As(V) breakthrough curves IOCS column experiment at pH 4.0 and As(V) fitted curves with equilibrium model (CDE) and nonequilibrium model (TSM) by using HYDRUS-1D model
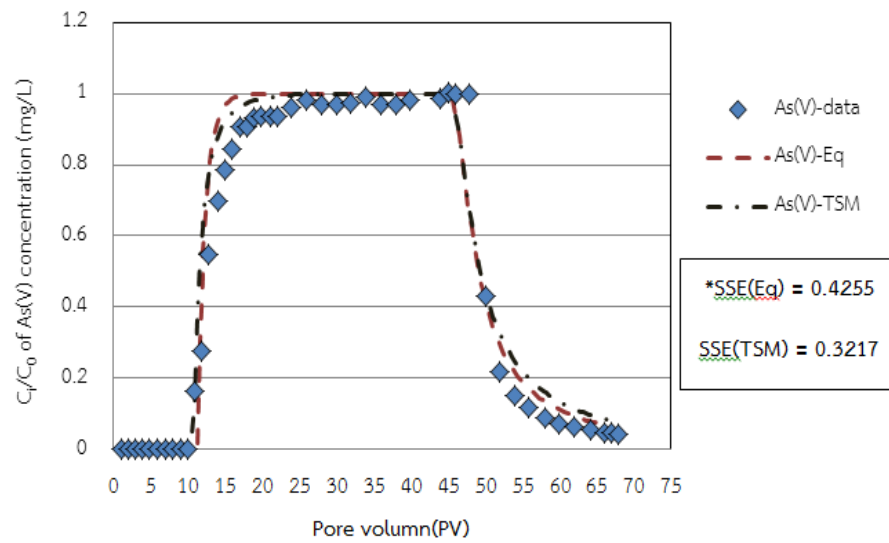
Figure 4.20-As(V) breakthrough curves from IOCS column experiment at pH 7.0 and As(V) fitted curves with equilibrium model (CDE) and nonequilibrium model (TSM) by using HYDRUS-1D model.
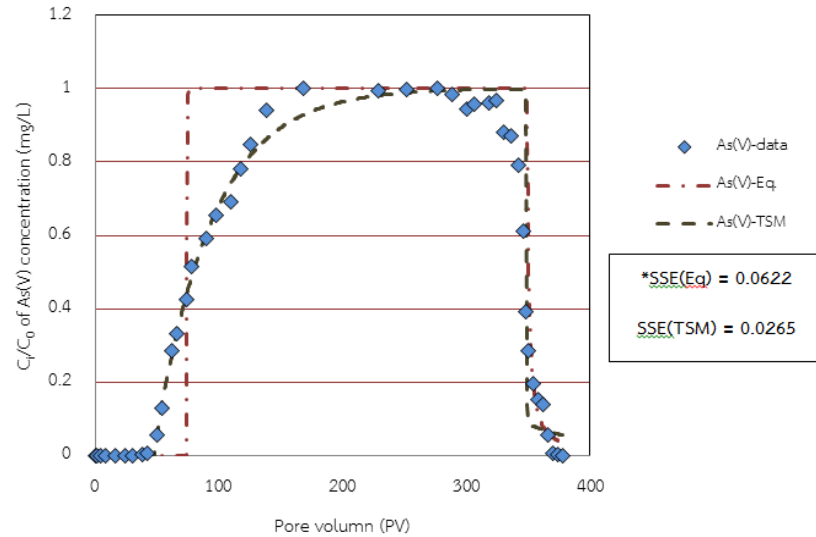
Figure 4.21-As(V) breakthrough curves from ZVICS-IOCS experiment at pH 4.0 and As(V) fitted curves with equilibrium model (CDE) and nonequilibrium model (TSM) by using HYDRUS-1D model.
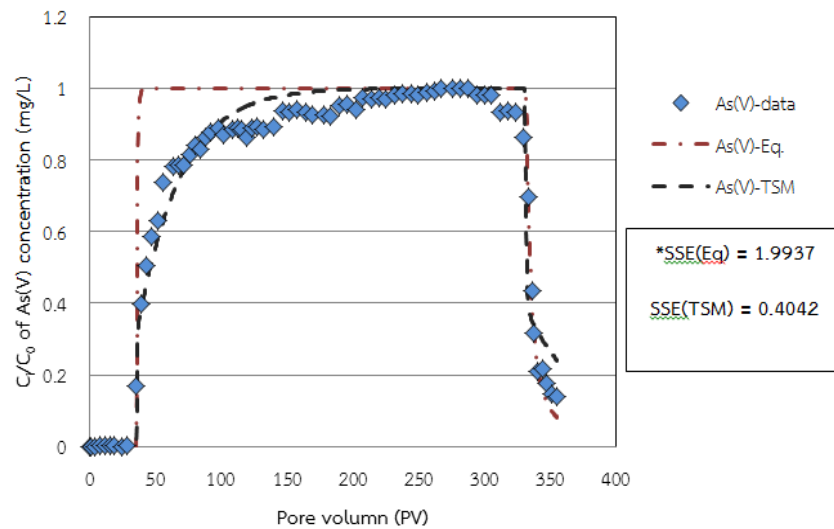
Figure 4.22-As(V) breakthrough curves from ZVICS-IOCS column experiment at pH 7.0 and As(V) fitted curves with equilibrium model (CDE) and nonequilibrium model (TSM) by using HYDRUS-1D model.

The As(V) fitted breakthrough curves with uniform (equilibrium) solute transport model and two-site model in column of sand, IOCS and ZVICS-IOCS with different pH solution (pH 4 and 7) as show in Figure 4.18-4.23.

Figures 4.17 and 4.18 show the fitted curves of sand column at pH 4 and 7. The fitted equilibrium transport model on sand column at pH (4 and 7) was closely with breakthrough curves from column experiment data. Table 4.8 shows estimated transport parameters for As(V) breakthrough curves from equilibrium convection-dispersion and non-equilibrium approaches(two-site model) generated by Hydrus-1D model.

According to Table 4.8, The results of SSE (sum of square error) values that calculated from equilibrium transport model in both pH 4 and 7 of sand column was less than the SSE values of the chemical non-equilibrium two-site model (TSM) (see Table 4.8). It was found that the curves fitted results of the uniform (equilibrium) transport model were significant.

Moreover, Figure 4.15 and 4.16 show the As(V) sorption capacity (mg/kg) onto sand pH (4 and 7). The results can confirm that the rate of As(V) adsorption onto sand column at pH (pH 4 and 7) have instantaneous adsorption. So, these results consistent with equilibrium solute transport model.

Figure 4.19-4.22 show fitted curves of IOCS at pH 4 and 7 and ZVICS and IOCS combination at pH 4 and 7. The results of fitted curves shows two-site model fitted curves were nearly with breakthrough curve derived from column experiments. The SSE (sum of square error) value (Table 4.8) can be summarized as below:

At pH 4

$SSE_{(tsm)}$ of IOCS and (ZVICS+IOCS) < $SSE_{(eq)}$ of IOCS and (ZVICS+IOCS)

At pH 7

$SSE_{(tsm)}$ of IOCS and (ZVICS+IOCS) < $SSE_{(eq)}$ of IOCS and (ZVICS+IOCS)

Mentioned results indicated that the As(V) adsorption onto IOCS and ZVICSS+IOCS is described by two site model. Moreover, the fraction of sorption sites (f) and also the mass transfer value (α) in each column have a less value, illustrating that such a smaller fraction sites and mass transfer values lead to less instantaneous

sorption, more kinetic sorption, and more pronounced tailing, and the arrival of solute to easier (Simuek et al., 2008).

The fitted TSM breakthrough curves of IOCS at pH 4 and 7 (Figure 4.19 and 4.20) described a better prediction of As(V) adsorption onto IOCS, which is indicated that As(V) can adsorb onto IOCS divided in to two sorption sites (so-called TSM model). One of the sorption sites is instantaneous sorption site, while the second sorption sites is kinetic sorption site (Chotpantarat et al., 2011).

The results of fitted TSM curves from HYDRUS-1D model concerning with the first kinetic adsorption rate. Such a model is lined with pervious study of Hsu et al. 2008 who studied removal of As(V) by using iron oxide coated sand (IOCS). The experiment used IOCS. Arsenic removal is explained by kinetic sorption isotherm. The experiment used dosage 24 g/L, control initial As(V) concentration 0.2 mg/L and varies pH condition (e.g.,5,6,7 and 8). The results of kinetic sorption isotherm show IOCS took around 6 hours to remove As(V) completely under four different pH conditions. Similarly, Lai et al. (2012) studied the adsorptive characteristics in a system consisting of iron-coated sands and arsenic solution. The kinetic adsorption experiment were used 2.5 g IOCS with various As(V) concentration 80 mg, 160 mg and 320 mg/L, pH of at 2.5, ionic strength of 0.01, pH at 25ºC and adsorption reaction time ranged from 2 to 2,880 min. The result of kinetic shows the sorption rate of As(V) on IOCS was completely fast in an initial time. After 20 minute, the As(V) had been adsorbed by IOCS about 48-78% and the adsorption of As(V) had approached to equilibrium

sorption after 60 min of contact time. The results show the adsorption capacity was increase to 90% and dramatically increase to 100% at the end of contact time 2,880 min. At nearly the end of contact time the As adsorption onto IOCS was gradually slowly adsorption rate and approach to equilibrium adsorption. Moreover, The R^2 value of the fitted curves shows that the pseudo-second order kinetic adsorption well fits the kinetic adsorption reactions of As(V) onto IOCS. At As(V) concentration 80 mg, 160 mg and 320 mg/, the equilibrium sorption capacity(q_e) were increased from 0.94 to 3.57 mg/g.

Consequently, the results of TSM fitted curves from HYDRUS-1D model and kinetic adsorption isotherm could implies that the mechanism of As(V) adsorption onto IOCS was divided in to two sorption sites instantaneous and kinetic sorption site.

According to Figures 4.15 and 4.16 show rate of As(V) adsorption in IOCS and mixing of ZVICS and IOCS column at pH 4 and 7. The result shows the kinetic rate of As(V) adsorption onto IOCS and ZVI coated sand combination with IOCS column at pH 4 and 7. Because of the heterogeneous adsorbent surface (see Figure 4.15 and 4.16), sorption to some surfaces may not be in equilibrium (Chotpantarat et al., 2011).

According to the study of Wang et al. (2006), they studies the removal of As(V) and As(III) by using zero-valent iron (ZVI) powder with ZVI concentration of 2.5 g/L. The concentration of As(V) was varied in two levels (0.1 mg/L and 0.5 mg/L) and the control system sealed (anaerobic) or unsealed (aerobic). For the two arsenic concentration levels of this experiment, removal process of both As(V) and As(III) conformed to the

first-order kinetics. In aerobic system, over 95% of As(V) was adsorbed on ZVI in 4 hours for both 0.1 mgAs/L and 0.5 mgAs/L, while As(III) was removed in the same period about 60%. The reaction rate constants (k) of As(V) removal was 0.348 and 0.367 at 0.5 mgAs /L and 0.1 mg/L, respectively. The k results of As(V) removal were better than the reaction rate constants (k) of As(III) (0.5 mgAs/L: 0.223, 0.1 mg/L: 0.243). However, As(III) could be remove in high level when time is enough, with 95% removal efficiency in 16 hours for two level (0.5 mgAs/L and 0.1 mg/L).

On the other hand, this experiment found that As in both As(V) and As(III) could be removed more efficiency in aerobic condition, especially for As(V). This might be attributed to adsorption of arsenic to iron and its corrosion products because of the interaction between As compounds and iron oxyhydroxides (FeOOH).

So, the results of their studies may conform to the result of As(V) adsorption onto ZVICS-IOCS combination fitted TSM curves by using HYDRUS-1D model. The results of kinetic sorption could confirm that the site of adsorbent divided into two fractions (e.g. instantaneous and kinetic sorption sites.

CHAPTER V
CONCLUSIONS AND RECOMMENDATIONS

5.1 Effect of pH on removal of As (V) in column experiment

- The removal capacity of As(V) increases with decreasing pH solution.

- The As(V) was removed most favorably under condition of acidic environment

- pH_{zpc} of sand, IOCS and ZVICS-IOCS are 5.0,7.0 and 7.5, respectively.

- The retardation factor and removal capacity of sand, IOCS and ZVICS-IOCS were increases with decreasing pH and coating sand with iron oxide and zero-valent iron was increase As(V) adsorption site

- Higher pH solution favors the formation of negative surface charged onto surface, leading to lower adsorption of As(V) onto the surface of reactive materials (Sand, IOCs, ZVICS-IOCS).

5.2 SEM Image

- The surface of IOCS showed observable tetragonal structures of goethite on a surface. The pore size was increased by coating the crystalline goethite on sand surface. In addition, the specific surface area of IOCS (0.78 M^2/g larger than that of uncoated sand.

- SEM image of IOCS-ZVICS combination collected column showed the highest removal capacities of As(V) compared to IOCs alone. In addition, the descending

order of specific surface area of ZVICS, IOCS and uncoated sand is 0.81, 0.78 and n/A M^2/g

5.3 HYDRUS-1D model

- The mechanism of As(V) adsorption onto sand at pH 4 and pH 7 correspond to the uniform (equilibrium) solute transport model.

- The mechanism of As(V) adsorption onto IOCS at pH 4 and pH 7 correspond to the chemical non-equilibrium two-site model (TSM) with instantaneous site of 0.55-0.90.

- The mechanism of As(V) adsorption onto ZVICS-IOCS at pH 4 and pH 7 correspond to the chemical non-equilibrium two-site model (TSM) with instantaneous site of 0.01-0.08.

5.4 Recommendations

- The future study should consider the scaling effect (e.g., length of column and size of reactive materials), affecting on heavy metal transport through porous media.

- This thesis only focuses on As(V) removal onto IOCS and ZVICS combination with IOCS under various pH conditions. The future study should investigate other heavy metals and/or other environmental conditions.

REFERENCES

Choprapawon, C., Ajjimangkul, S., Calderon, W. R., Chappell, C. O., & Abernathy, R. L. (1999). Major Interventions on Chronic Arsenic Poisoning in Ronpibool District, Thailand—Review and Long-Term Follow Up *Arsenic Exposure and Health Effects III* (pp. 355-362). Oxford: Elsevier Science Ltd.

Chotpantarat, S., Ong, S. K., Sutthirat, C., & Osathaphan, K. (2011). Effect of pH on transport of Pb^{2+}, Mn^{2+}, Zn^{2+} and Ni^{2+} through lateritic soil: Column experiments and transport modeling. *Journal of Environmental Sciences, 23*(4), 640–648.

Dhagat, A., B, G., & Sailo, L. (2013). Effect of Size of Iron Oxide Coated Sand (IOCS) on Removal of Cr (VI) from Water. *Proceedings Environmental and Biological Sciences (ICEEBS'2013)*, 29-30.

Eisazadeh, A., Eisazadeh, H., & Kassim, K. A. (2013). Removal of Pb(II) using polyaniline composites and iron oxide coated natural sand and clay from aqueous solution. *Synthetic Metals, 171*, 56–61.

Gebreyowhannes, Y.B. 2009. Effect of Silica and pH on Arsenic Removal by Iron-Oxide Coated Sand. Master's thesis, Institute for Water Education, 66 pp.

Genc-Fuhrman, H., Bregnhøj, H., & McConchie, D. (2005). Arsenate removal from water using sand–red mud columns. *Water Research, 39*, 2944–2954.

Gupta, V. K., Saini, V. K., & Jain, N. (2005). Adsorption of As(III) from aqueous solutions by iron oxide-coated sand. *Journal of Colloid and Interface Science, 288*(1), 55–60.

Han, R., Zou, W., Zhang, Z., Shi, J., & Yang, J. (2006). Removal of copper(II) and lead(II) from aqueous solution by manganese oxide coated sand I. Characterization and kinetic study. *Journal of Hazardous Materials, B137*, 384–395.

Han, Y.-S., Gellegos, T. J., Demond, A. H., & Hayes, K. F. (2011). FeS-coated sand for removal of arsenic(III) under anaerobic conditions in permeable reactive barriers. *Water Research, 45*(2), 593-604.

Henderson, A., & Demond, A. H. (2007). Long-termperformance of zero-valent ironpermeable reactive barriers: a critical review. *EnvironEng Sci, 24*, 401-423.

Hsu, J.-C., Lin, C.-J., Liao, C.-H., & Chen, S.-T. (2008). Removal of As(V) and As(III) by reclaimed iron-coated coated sands. *Journal of Hazadous Materials, 153*, 817-826.

Kamolpornwijit, W., Liang, L. Y., West, O. R., Moline, G. R., & Sullivan, A. B. (2003). Preferential flow path development and its influence on long-term PRB performance: column study. *Journal of Contaminant Hydrology, 66*(3-4), 161-178.

Lai, C.-H., Chen, C.-Y., Wei, B.-L., & Yeh, S.-H. (2002). Cadmium adsorption on goethite-coated sand in the presence of humic acid. *Water Research, 36*, 4943–4950.

Lee, C.-L., & Jou, G. C.-J. (2013). Removal of chlorobenzene using cordiarite coated with zero-valent iron under microwave irradiation. *Sustain. Environ. Res., 23*(6), 421-426.

Maji, K. S., Kao, Y.-H., Liao, P.-Y., Lin, Y.-j., & Liu, C.-W. (2013). Implementation of the adsorbent iron-oxide-coated natural rock(IOCNR) on synthetic As(III) and on real arsenic-bearing sample with filter. *Applied Surface Science, 284*, 40-48.

Mak, S. H. M., Lo, M. C. I., & Liu, T. (2011). Synergistic effect of coupling zero-valent iron with iron oxide-coated sand in columns for chromate and arsenate removal from groundwater: Influences of humic acid and the reactive media configuration. *Water Research, 45*, 6575-6584.

Mak, S. H. M., Rao, P., & Lo, M. C. I. (2011). Zero-valent iron and iron oxide-coated sand as a combination for removal of co-present chromate and arsenate from groundwater with humic acid. *Environment Pollution, 159*, 377-382.

Mohan, D., & J, P. (2007). Arsenic Removal from Water/Wastewater using Adsorbents--A critical review. *Journal of Hazardous Materials, 142*(1-2), 1-53.

Nova scotia environment, The drop on water Arsenic. [Online]. 2008. Available from http://www.novascotia.ca/nse/water/docs/droponwaterFAQ_Arsenic.pdf.

Petrusevski, B., Meer, W., Baker, J., Kruis, F., Sharma, S., & Schippers, J. (2007). Innovative approach for treatment of arsenic contaminated ground water in Central

Europe Proceedings 8th IWA Regional conference: Ground water Management in the Danube Basin and other Large river basins, Belgrade, Serbia.

Petrusevski, B., Sharma, S., Meer, W., Kruis, F., Khan, M., Barua, M., & JC, S. (2008). Four years development and field-testing of IHE Arsenic Removal Family Filter in rural Bangladesh." Proceedings 8[th]IWA Speciakized Conference on small water and wastewater systems, coimbatore, India.

Rahman, M. M., Begum, Z. A., Sawai, H., Maki, T., & Hasegawa, H. (2013). Decontamination of spent iron-oxide coated sand from filters used in arsenic removal *Chemosphere, 92*(2), 196-200.

Selim, H.M., J.M. Davidson, and R.S. Mansell. 1976. Evaluation of a two-site adsorption–desorption model for describing solute transport in soil. p. 444–448. *In* Proc. Summer Computer Simulation Conf., Washington,DC. 12–14 July 1976. Simulation Councils, La Jolla, CA.

Simunek, J., & Genuchten, M. T. v. (2008). Modeling Nonequilibrium Flow and Transport Processes Using HYDRUS. *Vodoze Zone*, 782-797.

Sun, Y.-P., Li, X.-q., Cao, J., Zhang, W.-x., & Wang, P. H. (2006). Characterization of zero-valent iron nanoparticles. *Advances in Colloid and Interface Science, 120*(1-3), 47-56.

Tanboonchuy, V., Hsu, J.-C., Grisdanurak, N., & Liao, C.-H. (2011). Gas-bubbled nano zero-valent iron process for high concentration arsenate removal. *Journal of Hazadous Materials, 186*, 2123-2128.

Toride, N., Leij, F. J., & van Genuchten, M. T. (1999). The CXTFIT code for estimating transport parameters from laboratory or field tracer experiments version 2.1. In: Research Report Vol. 137 of US Salinity Laboratory, Agricultural Research Service, US Department of Agriculture, Riverside, CA, USA.

Uzum, C., Shahwan, T., Eroglu, E. A., Lieberwirth, I., Scott, B. T., & Hallam, R. K. (2008). Application of zero-valent iron nanoparticles for the removal of aqueous Co^{2+}ions under various experimental conditions. *Chemical Engineering, 144*, 213–220.

Vaishya, R. C., & Gupta, S. K. (2006). Arsenic(V) Removal by Sulfate Modified Iron Oxide-Coated Sand (SMIOCS) in a Fixed Bed Column. *Water Qual. Res. J. Canada, 41*(2), 157-163.

Van Genuchten, M.Th ., and R.J. Wagenet. 1989. Two-site/two-region models for pesticide transport and degradation: Theoretical development and analytical solutions. Soil Sci. Soc. Am. J. 53:1303–1310.

Wang, C. B., & W.X, Z. (1997). Synthesizing nanoscale iron particles for rapid and complete dechlorination of TCE and PCBs. *Environ.Sci. Techno., 31*(7), 2154–2156.

WHO. Guidelines for drinking water quality, Vol 1: Recommendations. 2nd ed.; World Health Organization: Geneva. 2006.

Zhang, Y., & Gillham, R. W. (2005). Effects of gas generation and precipitates on performance of Fe^0 PRBs. *Ground Water, 43*(1), 113-121.

Zhou, d., Wang, D., Cang, L., Hao, X., & Chu, L. (2011). Transport and re-entrainment of soil colloids in saturated packed column: effects of pH and ionic strength. *Journal of Soil and Sediments, 11*, 491-503.

จุฬาลงกรณ์มหาวิทยาลัย
CHULALONGKORN UNIVERSITY

APPENDIX A

Column experiment data: Effect of pH 4 and pH 7 to As(V) transport through sand, IOCS and ZVICS-IOCS column

Table 1 - Observed breakthrough curve of As(V) through saturated sand column at pH 4

Sample (No.)	Pore volumn (PV)	C_i (ppm)	C_0 (ppm)	C_i/C_0
1	1	0.0002	10.713	1.87E-05
2	2	0.0004	10.713	3.73E-05
3	3	0.0003	10.713	2.80E-05
4	4	0.001	10.713	9.33E-05
5	5	0.0019	10.713	1.77E-04
6	6	0.0024	10.713	2.24E-04
7	7	0.646	10.713	6.03E-02
8	8	3.3853	10.713	3.16E-01
9	9	5.4213	10.713	5.06E-01
10	11	8.8112	10.713	8.22E-01
11	13	9.9814	10.713	9.32E-01
12	15	10.1645	10.713	9.49E-01
13	17	9.8636	10.713	9.21E-01
14	19	10.0448	10.713	9.38E-01
15	23	10.1431	10.713	9.47E-01
16	25	10.067	10.713	9.40E-01
17	27	10.4257	10.713	9.73E-01
18	29	10.4869	10.713	9.79E-01
19	31	10.7804	10.713	1.01E+00
20	33	10.484	10.713	9.79E-01
21	35	10.4494	10.713	9.75E-01
22	37	10.4153	10.713	9.72E-01
23	39	10.5583	10.713	9.86E-01
24	41	10.3974	10.713	9.71E-01
25	43	10.583	10.713	9.88E-01
26	46	10.6884	10.713	9.98E-01
27	47	10.7137	10.713	1.00E+00
28	49	10.1645	10.713	9.49E-01
29	51	9.9814	10.713	9.32E-01

Sample (No.)	Pore volumn (PV)	C_i (ppm)	C_0 (ppm)	C_i/C_0
30	53	9.8112	10.713	9.16E-01
31	55	8.7213	10.713	8.14E-01
32	57	6.7244	10.713	6.28E-01
33	58	0.5432	10.713	5.07E-02
34	59	0.029	10.713	2.71E-03
35	60	0.019	10.713	1.77E-03
36	61	0.0013	10.713	1.21E-04
37	62	0.0003	10.713	2.80E-05

Table 2 - Observed breakthrough curve of As(V) through saturated sand column at pH 7

Sample (No.)	Pore volumn (PV)	C_i (ppm)	C_0 (ppm)	C_i/C_0
1	1	0.0027	9.5835	0.0003
2	2	0.0031	9.5835	0.0003
3	3	0.0038	9.5835	0.0004
4	4	0.0053	9.5835	0.0006
5	5	0.5783	9.5835	0.0603
6	6	6.8421	9.5835	0.7139
7	7	8.6673	9.5835	0.9044
8	8	8.7277	9.5835	0.9107
9	9	9.1277	9.5835	0.9524
10	10	8.9975	9.5835	0.9389
11	11	9.4093	9.5835	0.9818
12	12	9.2694	9.5835	0.9672
13	13	9.4347	9.5835	0.9845
14	14	9.3005	9.5835	0.9705
15	15	9.2628	9.5835	0.9665
16	16	9.0975	9.5835	0.9493
17	17	9.3554	9.5835	0.9762
18	18	9.22	9.5835	0.9621
19	19	9.1306	9.5835	0.9527

Sample (No.)	Pore volumn (PV)	C_i (ppm)	C_0 (ppm)	C_i/C_0
20	20	9.3385	9.5835	0.9744
21	21	9.4542	9.5835	0.9865
22	22	9.4678	9.5835	0.9879
23	23	9.3191	9.5835	0.9724
24	24	9.3032	9.5835	0.9708
25	25	8.9571	9.5835	0.9346
26	26	8.9913	9.5835	0.9382
27	27	8.9039	9.5835	0.9291
28	28	8.9694	9.5835	0.9359
29	29	8.9448	9.5835	0.9334
30	30	8.9571	9.5835	0.9346
31	33	0.544	9.5835	0.0568
32	37	0.1532	9.5835	0.0160
33	41	0.1243	9.5835	0.0130
34	45	0.086	9.5835	0.0090
35	49	0.0605	9.5835	0.0063
36	50	0.058	9.5835	0.0061
37	51	0.0558	9.5835	0.0058
38	52	0.0562	9.5835	0.0059

Table 3 - Observed breakthrough curve of As(V) through IOCS column at pH 4

Sample (No.)	Pore volumn (PV)	C_i (ppm)	C_0 (ppm)	C_i/C_0
1	0	0.0153	9.3433	0.00164
2	4	0.0107	9.3433	0.00115
3	8	0.0092	9.3433	0.00098
4	12	0.0111	9.3433	0.00119
5	16	0.0127	9.3433	0.00136
6	20	3.1697	9.3433	0.33925
7	24	5.4277	9.3433	0.58092
8	28	6.3924	9.3433	0.68417
9	32	6.7082	9.3433	0.71797
10	36	6.9467	9.3433	0.74350
11	40	7.4059	9.3433	0.79264
12	44	7.4102	9.3433	0.79310
13	48	7.4034	9.3433	0.79238
14	52	7.6926	9.3433	0.82333
15	56	7.9848	9.3433	0.85460
16	60	8.4756	9.3433	0.90713
17	64	8.4387	9.3433	0.90318
18	68	8.5204	9.3433	0.91193
19	72	8.5911	9.3433	0.91949
20	76	8.6145	9.3433	0.92200
21	80	8.5729	9.3433	0.91755
22	84	8.6098	9.3433	0.92149
23	88	8.6229	9.3433	0.92290
24	92	8.8569	9.3433	0.94794
25	96	8.8739	9.3433	0.94976
26	100	8.9648	9.3433	0.95949
27	104	8.9906	9.3433	0.96225
28	108	8.9906	9.3433	0.96225
29	112	9.0281	9.3433	0.96626
30	116	9.0956	9.3433	0.97349
31	120	9.1089	9.3433	0.97491
32	124	9.1092	9.3433	0.97494

Sample (No.)	Pore volumn (PV)	C_i (ppm)	C_0 (ppm)	C_i/C_0
33	128	9.1122	9.3433	0.97527
34	132	9.1124	9.3433	0.98897
35	180	9.2402	9.3433	0.99134
36	200	9.2624	9.3433	0.99544
37	220	9.3007	9.3433	0.99609
38	240	9.3068	9.3433	0.99641
39	260	9.3098	9.3433	0.98718
40	321	9.2235	9.3433	0.80010
41	360	7.4756	9.3433	0.76673
42	364	7.1638	9.3433	0.65970
43	368	6.1638	9.3433	0.14433
44	372	1.3485	9.3433	0.11133
45	376	1.0402	9.3433	0.08810
46	383	0.8231	9.3433	0.07770
47	384	0.726	9.3433	0.06731
48	388	0.6289	9.3433	0.05756
49	392	0.5378	9.3433	0.03580
50	396	0.3345	9.3433	0.03424
51	400	0.3199	9.3433	0.02795
52	408	0.2611	9.3433	0.02183
53	412	0.204	9.3433	0.02677
54	416	0.2501	9.3433	0.02106
55	420	0.1968	9.3433	0.02039
56	424	0.1905	9.3433	0.01937
57	428	0.181	9.3433	0.01875
58	432	0.1752	9.3433	0.01809
59	436	0.169	9.3433	0.01787
60	440	0.167	9.3433	0.01578
61	444	0.1474	9.3433	0.01519
62	448	0.1419	9.3433	0.01523
63	452	0.1423	9.3433	0.01471
64	456	0.1374	9.3433	0.01450

Sample (No.)	Pore volumn (PV)	C_i (ppm)	C_0 (ppm)	C_i/C_0
65	460	0.1355	9.3433	0.01450
66	464	0.1308	9.3433	0.01400
67	468	0.126	9.3433	0.01349
68	472	0.123	9.3433	0.01316
69	476	0.1246	9.3433	0.01334

Table 4 - Observed breakthrough curve of As(V) through IOCS column at pH 7

Sample (No.)	Pore volumn (PV)	C_i (ppm)	C_0 (ppm)	C_i/C_0
1	1	0.0024	8.2576	0.0003
2	2	0.0024	8.2576	0.0003
3	3	0.0023	8.2576	0.0003
4	4	0.0023	8.2576	0.0003
5	5	0.0021	8.2576	0.0003
6	6	0.0019	8.2576	0.0002
7	7	0.0018	8.2576	0.0002
8	8	0.0018	8.2576	0.0002
9	9	0.002	8.2576	0.0002
10	10	0.008	8.2576	0.0010
11	11	1.3448	8.2576	0.1629
12	12	2.259	8.2576	0.2736
13	13	4.4818	8.2576	0.5427
14	14	5.7638	8.2576	0.6980
15	15	6.4914	8.2576	0.7861
16	16	6.9565	8.2576	0.8424
17	17	7.4523	8.2576	0.9025
18	18	7.4636	8.2576	0.9038
19	19	7.7085	8.2576	0.9335
20	20	7.7165	8.2576	0.9345
21	21	7.7339	8.2576	0.9366
22	22	7.7414	8.2576	0.9375
23	24	7.9071	8.2576	0.9576

Sample (No.)	Pore volumn (PV)	C_i (ppm)	C_0 (ppm)	C_i/C_0
24	26	8.1021	8.2576	0.9812
25	28	8.0228	8.2576	0.9716
26	30	8.0005	8.2576	0.9689
27	32	8.0365	8.2576	0.9732
28	34	8.1918	8.2576	0.9920
29	36	7.9909	8.2576	0.9677
30	38	7.9965	8.2576	0.9684
31	40	8.0789	8.2576	0.9784
32	44	8.1329	8.2576	0.9849
33	45	8.2721	8.2576	1.0018
34	46	8.2476	8.2576	0.9988
35	48	8.2471	8.2576	0.9987
36	50	3.5518	8.2576	0.4301
37	52	1.8275	8.2576	0.2213
38	54	1.2191	8.2576	0.1476
39	56	0.9482	8.2576	0.1148
40	58	0.7112	8.2576	0.0861
41	60	0.604	8.2576	0.0731
42	62	0.5155	8.2576	0.0624
43	64	0.4501	8.2576	0.0545
44	66	0.3839	8.2576	0.0465
45	67	0.3804	8.2576	0.0461
46	68	0.3397	8.2576	0.0411

Table 5 - Observed breakthrough curve of As(V) through mixing of ZVICS and IOCS column at pH 4

Sample (No.)	Pore volume (PV)	C_i (ppm)	C_0 (ppm)	C_i/C_0 (ppm)
1	0	0.0001	0.0001	7.836E-06
2	1	0.0003	0.0003	2.351E-05
3	4	0.0006	0.0006	4.702E-05
4	8	0.0007	0.0007	5.485E-05
5	12	0.0007	0.0007	5.485E-05
6	16	0.0012	0.0012	9.404E-05
7	20	0.0028	0.0028	2.194E-04
8	24	0.0052	0.0052	4.075E-04
9	30	0.0078	0.0078	6.112E-04
10	34	0.0327	0.0327	2.562E-03
11	38	0.0562	0.0562	4.404E-03
12	42	0.0781	0.0781	6.120E-03
13	46	0.0807	0.0807	6.324E-03
14	50	0.7137	0.7137	5.593E-02
15	54	1.6583	1.6583	1.300E-01
16	58	2.7889	2.7889	2.185E-01
17	62	3.6356	3.6356	2.849E-01
18	66	4.2638	4.2638	3.341E-01
19	70	5.0859	5.0859	3.986E-01
20	74	5.439	5.439	4.262E-01
21	78	6.5899	6.5899	5.164E-01
22	82	6.9654	6.9654	5.458E-01
23	86	7.2236	7.2236	5.661E-01
24	90	7.5541	7.5541	5.920E-01
25	94	8.1208	8.1208	6.364E-01
26	98	8.3505	8.3505	6.544E-01
27	102	8.5157	8.5157	6.673E-01
28	106	8.5297	8.5297	6.684E-01
29	110	8.8334	8.8334	6.922E-01
30	114	9.1686	9.1686	7.185E-01
31	118	9.9616	9.9616	7.806E-01
32	121	10.2752	10.2752	8.052E-01

Sample (No.)	Pore volume (PV)	C_i (ppm)	C_0 (ppm)	C_i/C_0 (ppm)
33	122	10.1921	10.1921	7.987E-01
34	126	10.8266	10.8266	8.484E-01
35	130	11.0072	11.0072	8.626E-01
36	134	11.9408	11.9408	9.357E-01
37	138	12.0303	12.0303	9.427E-01
38	140	11.8302	11.8302	9.271E-01
39	142	12.2604	12.2604	9.608E-01
40	152	12.2823	12.2823	9.625E-01
41	156	12.3143	12.3143	9.650E-01
42	160	12.3562	12.3562	9.683E-01
43	162	12.5911	12.5911	9.867E-01
44	164	12.5651	12.5651	9.846E-01
45	168	12.7528	12.7528	9.994E-01
46	176	12.3525	12.3525	9.680E-01
47	185	12.2983	12.2983	9.637E-01
48	189	12.5947	12.5947	9.870E-01
49	193	12.417	12.417	9.730E-01
50	199	12.6736	12.6736	9.932E-01
51	201	12.6051	12.6051	9.878E-01
52	211	12.193	12.193	9.555E-01
53	217	12.1894	12.1894	9.552E-01
54	223	12.2263	12.2263	9.581E-01
55	229	12.6968	12.6968	9.950E-01
56	235	12.8396	12.8396	1.006E+00
57	241	12.6875	12.6875	9.942E-01
58	246	12.857	12.857	1.008E+00
59	252	12.7286	12.7286	9.975E-01
60	258	12.6896	12.6896	9.944E-01
61	264	12.68	12.68	9.937E-01
62	270	12.4385	12.4385	9.747E-01
63	276	12.7675	12.7675	1.001E+00
64	282	12.8824	12.8824	1.010E+00
65	288	12.5545	12.5545	9.838E-01
66	294	12.389	12.389	9.708E-01

Sample (No.)	Pore volume (PV)	C_i (ppm)	C_0 (ppm)	C_i/C_0 (ppm)
67	300	12.0638	12.0638	9.454E-01
68	306	12.2237	12.2237	9.579E-01
69	318	12.2499	12.2499	9.599E-01
70	324	12.3506	12.3506	9.678E-01
71	330	11.2634	11.2634	8.826E-01
72	336	11.1214	11.1214	8.715E-01
73	342	10.0793	10.0793	7.899E-01
74	346	7.823	7.823	6.130E-01
75	348	5.0165	5.0165	3.931E-01
76	350	3.6554	3.6554	2.865E-01
77	354	2.5219	2.5219	1.976E-01
78	358	1.9727	1.9727	1.546E-01
79	362	1.8029	1.8029	1.413E-01

Table 6 - Observed breakthrough curve of As(V) through mixing of ZVICS and IOCS column at pH 7

Sample (No.)	Pore volume (PV)	C_i (ppm)	C_0 (ppm)	C_i/C_0 (ppm)
1	1	0.0007	9.7298	0.00007
2	4	0.0017	9.7298	0.00017
3	8	0.0045	9.7298	0.00046
4	12	0.0058	9.7298	0.00060
5	16	0.0072	9.7298	0.00074
6	20	0.0079	9.7298	0.00081
7	24	0.0083	9.7298	0.00085
8	28	0.00117	9.7298	0.00012
9	32	0.0126	9.7298	0.00129
10	40	1.5993	9.7298	0.16437
11	44	3.8508	9.7298	0.39577
12	48	4.8755	9.7298	0.50109
13	52	5.6758	9.7298	0.58334
14	56	6.098	9.7298	0.62673
15	60	7.1975	9.7298	0.73974

Sample (No.)	Pore volume (PV)	C_i (ppm)	C_0 (ppm)	C_i/C_0 (ppm)
16	68	7.5900	9.7298	0.78008
17	72	7.6715	9.7298	0.78845
18	76	7.6725	9.7298	0.78856
19	80	7.9287	9.7298	0.81489
20	84	8.16	9.7298	0.83866
21	88	8.0916	9.7298	0.83163
22	92	8.4066	9.7298	0.86401
23	96	8.5222	9.7298	0.87589
24	102	8.6393	9.7298	0.88792
25	106	8.4492	9.7298	0.86838
26	112	8.596	9.7298	0.88347
27	116	8.6235	9.7298	0.88630
28	120	8.5657	9.7298	0.88036
29	124	8.4236	9.7298	0.86575
30	128	8.6499	9.7298	0.88901
31	132	8.6626	9.7298	0.89032
32	136	8.596	9.7298	0.88347
33	144	8.6868	9.7298	0.89280
34	150	9.0838	9.7298	0.93361
35	156	9.0466	9.7298	0.92978
36	162	9.143	9.7298	0.93969
37	168	9.0687	9.7298	0.93205
38	174	9.028	9.7298	0.92787
39	182	9.0064	9.7298	0.92565
40	188	8.9823	9.7298	0.92317
41	194	9.264	9.7298	0.95213
42	200	9.2934	9.7298	0.95515
43	206	9.1448	9.7298	0.93988
44	212	9.4776	9.7298	0.97408
45	218	9.4206	9.7298	0.96822
46	224	9.464	9.7298	0.97268
47	230	9.4271	9.7298	0.96889
48	236	9.5031	9.7298	0.97670
49	242	9.5892	9.7298	0.98555

Sample (No.)	Pore volume (PV)	C_i (ppm)	C_0 (ppm)	C_i/C_0 (ppm)
50	248	9.5627	9.7298	0.98283
51	254	9.5403	9.7298	0.98052
52	260	9.6117	9.7298	0.98786
53	266	9.6462	9.7298	0.99141
54	272	9.7185	9.7298	0.99884
55	280	9.7146	9.7298	0.99844
56	286	9.7169	9.7298	0.99867
57	292	9.722	9.7298	0.99920
58	298	9.5216	9.7298	0.97860
59	304	9.5301	9.7298	0.97948
60	310	9.5351	9.7298	0.97999
61	316	9.0365	9.7298	0.92874
62	322	9.0908	9.7298	0.93433
63	328	9.0468	9.7298	0.92980
64	334	8.4066	9.7298	0.86401
65	338	6.7714	9.7298	0.69594
66	340	4.2416	9.7298	0.43594
67	342	3.0719	9.7298	0.31572
68	344	2.0615	9.7298	0.21187
69	348	2.0633	9.7298	0.21206
70	352	1.7141	9.7298	0.17617
71	356	1.4273	9.7298	0.14669
72	359	1.3282	9.7298	0.13651

APPENDIX B

Microwave digestion: Average sorption capacity (mg/kg) of As(V) transport through sand, IOCS and ZVICS-IOCS column with pH 4 and pH 7
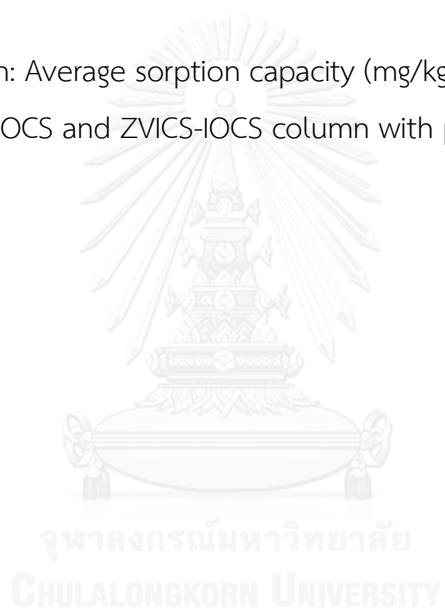
Table.7-Average sorption capacity of As(V) transport through sand, IOCS and ZVICS-IOCS column with pH 4

	Sand (mg/kg)	IOCS (mg/kg)	ZVICS-IOCS (mg/kg)
	0.4595	9.6432	31.4496
	0.4936	8.8372	23.1177
	0.5050	10.0485	31.1352
	0.4835	9.1656	26.1241
	0.5441	8.1880	28.8902
Average sorption capacity (mg/kg)	0.4972	9.1765	28.1433

Table.8-Average sorption capacity of As(V) transport through sand, IOCS and ZVICS-IOCS column with pH 7

	Sand (mg/kg)	IOCS (mg/kg)	ZVICS-IOCS (mg/kg)
	0.0566	5.4842	23.7667
	0.0549	4.0774	19.4223
	0.0576	4.2292	16.8697
	0.0777	3.0374	20.3107
	0.2348	4.2827	14.7709
Average sorption capacity (mg/kg)	0.0963	4.2222	19.0281

APPENDIX C

Point of zero charge (pH$_{zpc}$) of reactive materials (IOCS and ZVICS-IOCS)
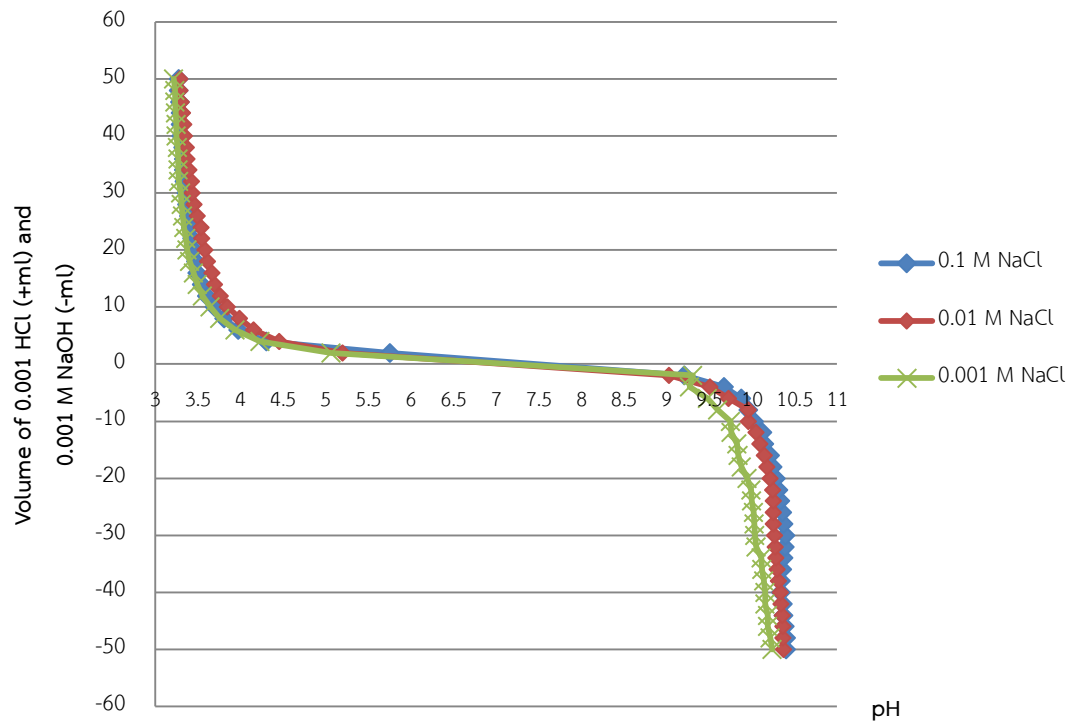
Figure 1-point of zero chart (pH$_{zpc}$) of IOCS surface

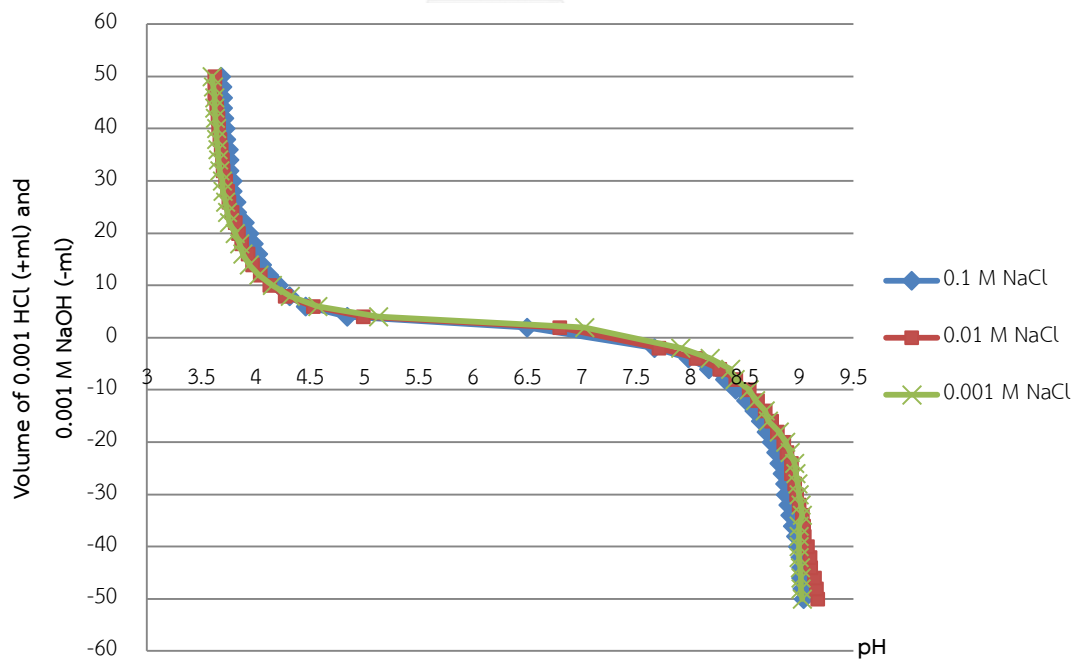**Figure 2**-point of zero chart (pH$_{zpc}$) of ZVICS surface

VITA

NAME: Miss.Chonnikarn Amasvata

DATE OF BIRTHDAY: 2nd February 1990

PLACE OF BIRTHDAY: Chachoengsao, Thailand

HOME ADDRESS: 184 Prachasan Road, Tabol Namueng, Amphoe Mueng, Chachoengsao 24000

CELL PHONE: +66(0) 880088420

E-MAIL: ka_pud@hotmail.com

EDUCATION: Bachelor of Science (Environmental Science), Chulalongkorn University, Thailand; 2009-2012

RESEARCH EXPERIENCE: Removal of cadnium from synthetic wastewater using activated carbon made from cashew nut shells.